A dual-activity topoisomerase complex regulates translation and abundance of mRNAs important for psychiatric disorders

Shuaikun Su
National Institute on Aging, NIH
Yutong Xue
Alexei Sharov
National Institute on Aging
Yongqing Zhang
NIA/NIH
Seung kyu Lee
National Institute on Aging
Jennifer Martindale
Wen Li
Peking University
Wai Lim Ku
NHLBI, NIH https://orcid.org/0000-0002-8859-6771
Keji Zhao
National Institutes of Health https://orcid.org/0000-0001-5559-6233
Supriyo De
National Institute on Aging, NIH
Payel Sen
National Institute on Aging, NIH https://orcid.org/0000-0003-2809-0901
Myriam Gorospe
National Institutes of Health
Dongyi Xu
Peking University https://orcid.org/0000-0001-5711-2618
Weidong Wang (wangw@grc.nia.nih.gov)
National Institute on Aging https://orcid.org/0000-0002-0658-7928

Research Article

Keywords: Topoisomerase, transcription, translation, TOP3B, TDRD3, FMRP, autism, CHD8

Posted Date: March 25th, 2022

DOI: https://doi.org/10.21203/rs.3.rs-1054387/v2

A dual-activity topoisomerase complex regulates translation and abundance of mRNAs important for psychiatric disorders

Shuaikun Su[1], Yutong Xue[1], Alexei Sharov[1], Yongqing Zhang[1], Seung Kyu Lee[1], Jennifer L. Martindale[1], Wen Li[3], Wai Lim Ku[2], Keji Zhao[2], Supriyo De[1], Payel Sen[1], Myriam Gorospe[1], Dongyi Xu[3] and Weidong Wang[1*]

[1] Laboratory of Genetics and Genomics, National Institute on Aging, Intramural Research Program, National Institute of Health, Baltimore, MD 21224, USA

[2]System Biology Center, National Heart, Lung and Blood Institute, National Institutes of Health, Bethesda, MD 20892, USA

[3]State Key Laboratory of Protein and Plant Gene Research, School of Life Sciences, Peking University, Beijing 1000871, China

*To whom correspondence should be addressed. Tel: +410-558-8334; Fax: +410-558-8331; Email: wangw@grc.nia.nih.gov

ABSTRACT

Topoisomerase 3b (TOP3B)-TDRD3 is a dual-activity topoisomerase complex in animals that can change topology for both DNA and RNA. A current hypothesis proposes that this complex interacts with Fragile X mental retardation protein, FMRP, to regulate mRNA translation. Here we examined this hypothesis by identifying TOP3B-TDRD3-bound mRNAs in human HCT116 cells; and analyzing the effect of inactivating TOP3B, TOP3B catalytic activity, TDRD3, and FMRP, on translation and abundance of these mRNAs. We found that TOP3B-TDRD3 resembles FMRP in preferentially binding to coding regions of long mRNAs. Complete inactivation of TOP3B protein, but not a point mutation that only disrupts TOP3B catalytic activity, preferentially reduced the abundance of the TOP3B-TDRD3-bound mRNAs. Moreover, ablation of the complex or inactivation of TOP3B catalytic activity alters translation for some but not all TOP3B-TDRD3 bound mRNAs, suggesting that TOP3B-TDRD3 may solve topological problems for specific mRNAs. Finally, several schizophrenia and autism-risk genes are bound and regulated by TOP3B-TDRD3 in mRNA translation and abundance by topoisomerase activity dependent and independent manners. Our data suggest that TOP3B-TDRD3 can regulate mRNA translation and abundance by topoisomerase activity dependent or independent mechanisms; and disruption of this function could contribute to pathogenesis of psychiatric disorders in *TOP3B* mutation carriers.

INTRODUCTION

Topoisomerases are “magicians” of the DNA world, with critical roles in relieving topological stress produced during DNA replication, transcription, and chromosome segregation (1). Mutations in or deregulation of topoisomerases can cause defective development, lethality, and human diseases, such as neurological disorders and cancer (1). A fundamental question that has remained unanswered is whether RNA metabolism also produces topological stress that requires resolution by a topoisomerase. Recent discoveries that a Type IA topoisomerase in animals, TOP3B, is a dual-activity topoisomerase that can change topology of both DNA and RNA (2,3), have led to the hypothesis that RNA metabolism may indeed produce topological problems resolved by TOP3B (4). Moreover, the findings that the RNA topoisomerase activity is prevalent in Type IA topoisomerases in all domains of life (5) further suggest that RNA topological problems occur in a wide range of species that select for retention of RNA topoisomerase activity through millions of years of evolution (4).

The notion that TOP3B can act in both DNA and RNA metabolism is supported by accumulating evidence. For DNA, TOP3B has been shown to promote neuronal activity-dependent transcription in the mouse brain (6); and to be recruited to specific promoters by its partner, TDRD3, to reduce R-loops and maintain genome stability (7,8). For RNA, TOP3B is the only topoisomerase in animals containing a conserved RNA binding domain, RGG-box, which is critical for TOP3B binding to mRNAs (9), and catalyzing RNA topoisomerase reactions (3). TOP3B works with the siRNA machinery to promote heterochromatin formation and silencing of transposons (10); and promotes neural development (9). In addition, TOP3B possesses a nuclear export sequence that allows it to shuttle between nucleus and cytoplasm (2). Moreover, overexpression of a TOP3B mutant can produce cleavage complexes on both DNA and RNA in cells (11), suggesting that TOP3B can catalyze reactions on both types of nucleic acid *in vivo*. Notably, TOP3B has been recently shown to be required for replication of positive-strand RNA viruses including SARS-CoV2, raising the possibility that TOP3B could be a feasible antiviral target (12).

Indirect evidence supports a role of the TOP3B-TDRD3 complex in mRNA translation (2,3). First, the complex can biochemically and/or genetically interact with translation regulators, including Fragile-X mental retardation protein (FMRP) (2,3), and the exon-junction complex (EJC) (2,13). Second, TDRD3 itself has been suggested to regulate translation of some mRNAs (14). Third, a large fraction of TOP3B is localized in the cytoplasm, where it co-localizes with TDRD3 and FMRP in RNA stress granules (SGs) in response to cellular stress (2,3). SGs are compartments consisting of transiently inactivated mRNAs and translation machinery, which are formed as a cytoprotective mechanism to shut down non-essential translation during stress. Fourth, TOP3B co-fractionates with TDRD3 and FMRP in polyribosomes (2,3,5), whose mRNAs are under active translation. Finally, *TOP3B* mutations have been linked to multiple psychiatric and cognitive disorders, including schizophrenia and autism (2,15-17). This feature also resembles that of FMRP, with the Fragile X syndrome identified as the leading cause of autism (18). This has led to the proposal that TOP3B works with FMRP to regulate translation of mRNAs important for these

disorders (2,3). However, critical evidence has been lacking to show that ablation of TOP3B protein or inactivation of its catalytic activity can alter translation of mRNA bound by the topoisomerase.

This study aims to address three basic questions regarding the roles of the TOP3B-TDRD3 complex in mRNA translation. First, whether the absence of TOP3B or TDRD3 affects translation or not? Second, is the topoisomerase activity of TOP3B required for mRNA translation? Third, which mRNAs are directly bound by TOP3B? To address these questions, we generated *TOP3B* or *TDRD3* knock-out; and *TOP3B-Y336F* knock-in (loss-of-topoisomerase activity but retaining RNA binding activity) mutant HCT116 cell lines. Then we performed Ribo-seq, RNA-seq and PRO-seq to detect the levels of translation, mRNA abundance and transcription using these cell lines. Our data show that TOP3B mainly binds coding regions of long mRNAs, and its binding stabilizes these mRNAs. In addition, TOP3B-TDRD3 complex and its associated topoisomerase activity is needed for normal translation of some of its bound mRNAs. Finally, several mRNAs encoded by autism and schizophrenia risk genes are bound and regulated by the TOP3B-TDRD3 complex, indicating that their dysregulation could be a mechanism by which *TOP3B* mutation contributes to pathogenesis of psychiatric disorders.

MATERIALS AND METHODS

Cell lines

HCT116 cells were cultured in Dulbeccos' Modified Eagle Medium (DMEM, Thermo Fisher Scientific) supplemented with 10% fetal bovine serum (HyClone) and 1% antibiotics (Penicillin-Streptomycin, Sigma). For generation of the *TOP3B-KO* HCT116 cell lines, pX330 plasmid containing the guide RNA sequence was transfected in HCT116 cells. Eight to ten days later, single clones were selected for screening of absence of TOP3B protein and mutations at *TOP3B* genomic locus by Western blotting and genomic sequencing analysis, respectively. CRISPR-Cas9 mediated ablation of the *TDRD3* and *FMR1* was achieved with PX459 plasmid as the targeting vector (Addgene) (19). Guide RNA sequences were designed using the http://crispr.mit.edu website and cloned into the targeting vector. Plasmids containing the guide RNA sequence were transfected into cells using FuGENE HD (E2311; Promega). Twenty-four hours post-transfection, the cells were added with fresh medium containing 1 µg/mL puromycin (P8833-10MG, Sigma). After 48 ~72 hours, cells were diluted with new medium (without puromycin) into 96-well plate. After one week, cells from single clones were transferred to 24-well plate. Then, Western blotting and Sanger sequencing were used to screen for clones that lack the target protein and harbor mutations in the target genes. The HCT116 cell line expressing TOP3B catalytic point mutant protein (*TOP3B-Y336F*) was generated by a modified CRISPR-Cas9 gene editing strategy (19). A single-strand DNA template (100 nt) designed to produce Y336F mutant protein was synthesized by Integrated DNA Technologies company. Plasmid containing the guide RNA sequence and the DNA template were transfected into HCT116 cells using FuGENE HD. Clone selection and validation were performed as described above. The guide RNA and DNA template sequences are described in Table S9 and Figure S1.

Ribosome profiling and RNA sequencing

Ribosome profiling protocol was based on a published method (20) with small modifications. Briefly, about 5~10 × 10^6 HCT116 cells were cultured in 10 cm dish for 12~16 hours. Cycloheximide (2112S, New England Biolabs) was added to a final concentration of 100 µg/mL for 10 min. Cells were washed with 2 mL cold phosphate buffered saline (PBS) with CHX, and then were collected on ice. Cells were lysed in 400 µL polysome lysis buffer by trituration through a 25-gauge needle. After centrifugation, 100 µL cell of lysates were used to extract RNA with TRIzol (15596026, Invitrogen). Then, 5~10 µg RNA was used to purify mRNAs using oligo dT beads (61012, Invitrogen). The purified mRNAs were used for RNA-seq library preparation by following a published protocol (6). Three hundred microliters of cell lysates were used for ribosome profiling. One thousand units of RNase T1 (EN0541, Thermo Fisher Scientific) were added to the lysates, and incubated at 25 °C for 1 hour at 500 rpm rotation. Two thousand units of RNase inhibitor (AM2696, Thermo Fisher Scientific) were added to the lysates to stop the digestion. Ribosomes were collected by sedimentation through 0.9 mL 1 M sucrose cushion. RNAs were extracted from the purified ribosomes with TRIzol. Then, 24-34 nt RNA fragments were purified using a 15% TBE-Urea gel (Thermo Fisher Scientific). Ribosomal RNAs were removed from the purified RNA fragments with NEBNext rRNA Depletion Kit (E6310S, New England Biolabs). The ribosome-protected fragments (RPFs) were treated with T4 Polynucleotide Kinase (M0201S, New England Biolabs) at 37 °C for 30 minutes with 20 units RNase inhibitor. After precipitation with isopropanol, the RPFs were used to prepare library with NEBNext® Multiplex Small RNA Library Prep Set for Illumina (E7300S, New England Biolabs). The RNA-seq and Ribo-seq libraries were sequenced by using the Hi-seq 2000 system (Illumina).

Because RNase I digestion has been commonly used in Ribo-seq, we also attempted to use RNase I to digest polysomes. However, ribosomes from HCT116 cells were very sensitive to RNase I digestion, and we were unable to obtain high quality data of RPFs (data not shown). As an alternative, RNase T1 was used to digest polysomes to monosomes without loss of ribosomes (21).

eCLIP-seq

eCLIP-seq protocol was based on a previous publication (22) with some modifications. *TOP3B-KO* HCT116 cells were used as negative control instead of IgG. Five µg of TOP3B antibody (WH0008940M1-100UG, Sigma Aldrich) was used for immunoprecipitation. RNA 5' Pyrophosphohydrolase (RppH) (New England Biolabs) was used to replace Tobacco Acid Pyrophosphatase (TAP) to treat RNA. All other steps and reagents were identical as described in the published method (22).

PRO-seq

PRO-seq was performed as previously described (23). Briefly, HCT116 cells were seeded at a concentration that will enable them to reach ~80% confluency on a 15 cm plate in 24 hours. Cells (about 10-20 million) were then collected, permeabilized, and processed for PRO-seq.

RNA Immunoprecipitation

Cytoplasmic lysates of HCT116 cells were prepared in polysome extraction buffer (20 mM Tris-HCl at pH 7.5, 100 mM KCl, 5 mM $MgCl_2$ and 0.5% NP-40) containing protease and RNase inhibitors. The supernatants were incubated with protein A-Sepharose beads coated with TOP3B antibody (WH0008940M1-100UG, Sigma Aldrich) for 2 h at 4 °C. After three washes with ice-cold NT2 buffer (50 mM Tris-HCl at pH 7.5, 150 mM NaCl, 1 mM $MgCl_2$, 0.05% NP-40), bound RNAs were extracted from the beads using TRIzol and subjected to RT-qPCR (24).

Polysome profiling

Polysome profiling was performed as previously described (3,5). Briefly, 5×10^6 HCT116 cells were cultured in a 10 cm dish for 12~16 hours. CHX (2112S, New England Biolabs) was added to the medium to a final concentration of 100 μg/mL for 10 min. Cells were collected on ice and lysed in polysome extraction buffer (20 mM Tris-HCl at pH 7.5, 100 mM KCl, 5 mM $MgCl_2$ and 0.5% NP-40). After centrifugation, the lysate was separated through 10% to 50% sucrose gradients, 12 fractions were collected, and RNA extracted to perform RT-qPCR. The distribution of mRNAs was quantified by RT-qPCR analysis and plotted as a percentage of the specific mRNA in each fraction relative to the total amount of that mRNA in the gradient.

Nascent RNA extraction

Nascent RNA was extracted based on a previously published method (25). Briefly, $1\sim2\times10^7$ HCT116 cells were collected and washed two times with ice-cold PBS. The cell pellet was resuspended with 10 mL ice-cold Hypotonic Buffer (10 mM HEPES, pH 8.0; 10 mM KCl; 2 mM $MgCl_2$; 1 mM DTT, add before use.) and incubated on ice for 15 min. The cell suspension was centrifuged at 200 ×g for 10 min at 4 °C and the supernatant was discarded. The pellet was resuspended in 2 mL cold Hypotonic Buffer and then transferred into a precooled 2 mL Dounce tissue grinder. The cell suspension was homogenized with a tight pestle using 20 strokes. The nuclei were pelleted by centrifugation at 600 × g for 10 min at 4 °C, and the supernatant was discarded. The nuclei pellet was then washed twice with 1 mL ice-cold Nuclei Wash Buffer (10 mM HEPES, pH 8.0; 250 mM Sucrose; 1 mM DTT and 20 U/mL RNase inhibitor). 1 × NUN Buffer (with RNase-free water) was prepared by mixing 50% volume of 2 M urea solution (fresh and filtered) and 50% volume of ice-cold 2 × NUN Buffer (40 mM HEPES, pH 8.0; 15 mM MgCl2; 0.4 mM EDTA; 600 mM NaCl; 2% v/v NP-40) with DTT and RNase inhibitor. The nuclei were suspended and disrupted using 1 × NUN buffer by pipetting up and down vigorously for 10 times followed by incubation on a rotating wheel for 5 min at 4 °C. The chromatin was pelleted by centrifugation at 1000 x g for 3 min at 4 °C. The chromatin pellet was washed three times with 1 × NUN buffer at 4 °C. And 1 mL of TRIzol Reagent was added into chromatin pellet followed by vortex for 30 s. The homogenized sample was incubated for 5~10 min at 50 °C on a nutator to dissolve the chromatin pellet. Then the rest steps of RNA extraction are the same as the standard protocol of RNA purification using TRIzol. DNA contamination was removed with DNase I (AMPD1-

1KT, Sigma Aldrich). Then the RNA was purified with TRIzol. RT-qPCR was performed to detect the nascent RNAs with the primers amplifying the exon-intron junction.

RNA extraction and RT-qPCR

HCT116 cells were cultured in 6-well plates for 12~16 h. For CHX treatment groups, 100μg/mL CHX was added into the medium for 3 hours before extracting RNA. After removing the medium, 1 mL TRIzol (Invitrogen, 15596026) was added to the plate directly to lyse the cells. The cell lysate was transferred into 1.5 mL tubes. Two hundred μL chloroform was added into the lysate, vortexed, and followed by centrifugation at 18,000 × g for 10 min at 4 °C. The aqueous phase was transferred to a new tube. RNA was precipitated in 1.5-fold volume of 2-propanol together with 10% volume of 3 M sodium acetate. cDNA was synthesized from 1 μg RNA using Taqman Reverse Transcription Reagents (Applied Biosystems, N8080234). After 10-fold dilution, the cDNA was used as a template to perform qPCR with SYBR Green PCR Master Mix (Applied Biosystems, 4309155). The PCR primer sequences can be found in Table S9.

Western blot and antibodies

Whole cell lysates were prepared using RIPA buffer (10 mM Tris-HCl at pH 7.4, 150 mM NaCl, 1% NP-40, 1 mM EDTA, 0.1% SDS, 1 mM dithiothreitol) containing protease inhibitor (11697498001, Roche). The protein concentrations were measured using Bradford (#500-0205, Bio-Rad). 2 × Laemmli Sample Buffer with 5% β-Mercaptoethanol were added into the protein lysates. After boiling at 95 °C for 10 min, the protein lysates were separated on a 4–20% Mini-PROTEAN® TGX™ Gel (Bio-Rad) and transferred to nitrocellulose membrane using Trans-Blot® Turbo™ Transfer System (Bio-Rad). Incubations with primary antibodies to detect TOP3B (WH0008940M1-100UG, Sigma Aldrich), TDRD3 (5942S, Cell Signaling Technology), FMRP (MAB2160, Sigma Aldrich), CHD8 (ab114126, Abcam), FAT1 (A304-403A, Thermo Fisher), GAPDH (2118s, Cell Signaling Technology) and ACTB (ab8226, Abcam) were followed by incubations with appropriate secondary antibodies conjugated with HRP (GE Healthcare). Signals were developed using Enhanced Chemiluminescence (ECL).

Bioinformatics analysis

Ribo-seq data analysis was performed as previously published (20). Briefly, low-quality reads and the adapter sequence (AGATCGGAAGAGCACACGTCTGAACTCCAGTCAC) were removed by FASTX-Toolkit from FastQ files. Reads less than 25 nt were also removed by FASTX-Toolkit. The remaining reads were aligned to the rRNA reference (hg38) using the Bowtie short-read alignment program. The rRNA alignments were discarded and the unaligned reads were collected. The non-rRNA sequencing reads were aligned to the human genomic reference (hg38) using HISAT2 (26). The raw counts were generated using HTSeq-Counts (27). Then DESeq2 was used to identify the differentially expressed genes (DEGs) and generate the normalized counts (28). The genes with total counts (untreated and treated groups) less than 10 were filtered. The genes (Fold change > 1.5 and adjust *P*-value < 0.1) were identified as DEGs. The

bedGraph files were generated by deepTools (29) and normalized using RPKM. The bedGraph files were visualized using the Integrative Genomics Viewer (IGV) (30). RNA-seq reads were mapped to hg38 human genome with HISAT2 directly. Then other steps were similar to those of Ribo-seq. PRO-seq reads were mapped to human genome with Bowtie2 allowing maximum of 2 mismatches (31). The read counts from transcription start site (TSS) regions (-700 to +700 bp from TSS) of each gene were normalized and used as transcription levels. Since we focused on post-transcriptional regulation in our study, genes with PRO-seq level changes (fold change > 1.2-fold in two replicates) were considered as DEGs.

eCLIP-seq reads were mapped to the genome using TopHat. The read counts from each gene were calculated and normalized using a perl script. Genes with criterion (WT-IP_fpkm/WT-Input_fpkm > 1.5 and WT-IP_fpkm/TOP3B-KO-IP_fpkm > 1.5) in both biological replicates were selected as TOP3B eCLIP targets. RSeQC was used to analyze the read distribution of eCLIP-seq on introns, CDS, 5'UTR and 3'UTR (32).

RESULTS

Studying TOP3B-TDRD3 function by creating knockout and knock-in mutant cell lines

Human HCT116 cell line has been extensively used for studies of transcription and translation, including analyses of topoisomerase 1 and 2 (TOP1 and TOP2). Here we chose the same cells to study TOP3B-TDRD3, so that we can easily compare our findings with those from other studies. We generated isogenic HCT116 cell lines that are individually inactivated for *TOP3B* (*TOP3B-KO*); *TDRD3* (*TDRD3-KO*); the catalytic activity of TOP3B (*Y336F-KI*); or their interacting protein FMRP (*FMR1-KO*), using the CRISPR-Cas9 technology (Figure 1A-D & Figure S1A-E) (19). Genomic DNA sequencing revealed the occurrence of cleavage-directed frame-shift mutations in various *KO* clones (Figure S1), as well as the targeted homozygous Y336F-substitutions in the *KI* clone (Figure 1D). Western blotting confirmed the absence of each target protein in their respective *KO* cells (Figure 1B). We noticed that the protein level of TOP3B was lower in *TDRD3-KO* cells (~70% reduction); and TDRD3 protein level was also lower in *TOP3B-KO* cells (~70% reduction); but both were unchanged in *FMR1-KO* cells (Figure 1B), which is consistent with earlier observations that TOP3B and TDRD3 depends on each other for stability (7). We generated an additional *TOP3B-KO* clone (*KO2*) using a different guide RNA and found that it expresses a mutant protein carrying a partial deletion of the Toprim domain (Figure S1B and Figure S1C). Because this highly conserved domain is critical for topoisomerase activity (33), the mutant protein is expected to show loss of function and was used as an internal control in our translation studies (see below). Western blotting also confirmed the presence of the TOP3B-Y336F mutant protein in *Y336F-KI* cells (Figure 1C). We noticed that the level of Y336F was about 50% of that of wild type (*WT*) cells, suggesting that the catalytic reaction may help to stabilize TOP3B protein.

We have also attempted to study TOP3B function using siRNA depletion. However, RNA-seq showed that many genes downregulated in *TOP3B-KO* and *Y336F-KI* cells exhibited normal expression in siRNA-treated cells, even though TOP3B mRNA was depleted by 80% (data not shown), suggesting that the siRNA approach is not suitable for studying catalytic function of TOP3B. The data also argue that the effect observed in *Y336F-KI* cells should not be caused by 50% reduction of TOP3B protein.

We used the cell lines generated above to study the function of TOP3B-TDRD3 and FMRP in mRNA translation by Ribo-seq, and in mRNA level regulation by RNA-seq. Ribo-seq (or Ribosome profiling) monitors translation of mRNAs genome-wide by quantifying ribosome-protected RNA fragments (RPFs) (20). To identify mRNAs directly regulated by TOP3B-TDRD3, we performed eCLIP-seq (34) using a TOP3B antibody. Because TOP3B is a dual-activity topoisomerase that can regulate transcription (6,7), a possibility exists that the effect of TOP3B on translation and mRNA levels could be due to its effect on transcription. To distinguish the different effects of TOP3B, we performed PRO-seq to identify genes regulated by TOP3B at the transcriptional level, and then excluded these genes when we analyze the effect of TOP3B inactivation on translation and mRNA abundance. PRO-seq measures transcription levels by detecting the nascent transcripts produced by an active RNA polymerase II (23). The detailed analysis of the PRO-seq data and the roles of TOP3B-TDRD3 in transcription will be described elsewhere.

As a proof of validity of our assays, the levels of RPFs and RNA-seq for *TOP3B, TDRD3*, and *FMR1* genes were reduced in *TOP3B-KO1, TDRD3-KO* cells, and *FMR1-KO* respectively (Figure S2A-B & Figure S2D-E), consistent with absence of these proteins in their respective *KO* cells (Figure 1B). In contrast, the levels of the PRO-seq for the same three genes remained unchanged in their respective KO cells (Figure S2A and S2D), consistent with that the absence of these proteins are not due to reduced transcription, but due to nonsense-mediated decay of mRNAs containing the out-of-frame mutations generated by CRISPR-CAS9. In addition, no obvious difference was observed for *TOP3B* mRNA in *TOP3B-KO2* cells (Figure S2C), which is also consistent with the finding that these cells express a truncated TOP3B protein (Figure S1C).

TOP3B regulates translation and mRNA levels of specific genes

Scattered plot analysis of our Ribo-seq and RNA-seq data from both *TOP3B-KO1* (3 replicates) and *TOP3B-KO2* (2 replicates) cells revealed strong correlation between signals of *KO* cells and those of *WT* cells (R>0.9) (Figure S3A), indicating that TOP3B inactivation does not alter global mRNA translation or abundance. This conclusion is further supported by polysome profiling analysis (35), which showed that the proportion of mRNAs under active translation (in the polysome fractions) are indistinguishable between KO vs. WT cells (Figure S3B).

We noted that the levels of RPFs from either *WT* or *TOP3B-KO* cells correlated well with those of RNA-seq (R=0.80), but poorly with those of PRO-seq (R=0.25, Figure S3C), which are consistent with previous findings (36). The heatmaps below (Figure 6B-C and Figure 8A-B) also showed strong co-clustering

between RPFs and RNA-seq signals, but not with those of PRO-seq, in the *TOP3B-KO*, *TOP3B-Y336F* and *TDRD3-KO* cells. These data suggest that translation and mRNA levels are largely co-regulated with each other through post-transcriptional mechanisms.

We then investigated whether TOP3B inactivation can alter translation or abundance of specific mRNAs. Volcano plots revealed 478 differentially expressed genes (DEGs) by RNA-seq and 725 DEGs by Ribo-seq (Figure 2A and Table S2, fold change > 1.5, adjusted *P*-value < 0.1) between *TOP3B-KO* vs. *WT* cells. Examination of the 725 DEGs identified by Ribo-seq show that the percentage of decreased vs. increased genes are 41% vs. 59%, implying that TOP3B may affect translation either positively or negatively. Because translation of an mRNA is often affected by its transcription and degradation (37), some of these DEGs could be regulated by TOP3B at those steps rather than at translation *per se*. To identify mRNAs that were dependent on TOP3B for translation, we divided the decreased DEGs identified by Ribo-seq into 4 groups, based on whether these genes show concomitant decrease in RNA-seq (which reflects steady-state mRNA levels) and PRO-seq (which measures nascent transcript levels correlating with transcription) (Figure 2B & Table S3). Group 1 DEGs showed no concomitant decrease in RNA-seq and PRO-seq levels, which should represent genes regulated by TOP3B at translation level only. Group 2 DEGs exhibited decreased signals in RNA-seq, but no change in PRO-seq signals. This group consists of transcripts like *TOP3B* mRNA, whose decreased translation also reduces mRNA levels through no-go decay or nonsense-mediated decay mechanisms (38-40). The group may also contain genes whose translation reduction is due to decreased mRNA levels caused by accelerated mRNA degradation. Group 3 DEGs showed concomitant decrease in PRO-seq but no change in RNA-seq, whereas Group 4 DEGs showed decrease in both RNA-seq and PRO-seq (Figure 2B). The last two groups likely consist of genes regulated at the transcription step.

This analysis revealed that majority of the decreased DEGs belong to group I (61%) and II (18%), suggesting that TOP3B mainly acts post-transcriptionally to regulate translation and mRNA stability. Analysis of the increased DEGs obtained similar results, as the most of the DEGs also belong to post-transcriptional groups (I and II) (Figure 2B). The number of decreased DEGs in groups 1 and 2 was comparable to that of increased DEGs (178 vs. 237), supporting the notion that TOP3B can either or repress translation. Because we are interested in the functions of TOP3B in post-transcriptional regulation, we focused on DEGs of group 1 and 2 below.

TOP3B regulates translation of several mRNAs important for mental disorders

We analyzed 4 representative genes (*CHD8, SMC3, EML3* and *FAT1*) from groups 1 and 2, all of which exhibited no significant differences in PRO-seq (Figure 2C-D), suggesting that they are regulated by TOP3B at the post-transcriptional level. Among them, the RPF levels of *CHD8* and *SMC3* are significantly reduced (adjusted *P*-value<0.01) (Figure 2C-D), whereas their mRNA levels are slightly reduced, but the difference does not reach statistical significance, indicating that their translation efficiency is reduced in *TOP3B-KO* cells (Figure 2C-D). Similarly, the RPF levels of *EML3* is significantly increased, whereas its mRNA levels

remain unchanged, suggesting increased translation efficiency for this gene. Moreover, the RPF and mRNA levels of *FAT1* are both significantly increased in *TOP3B-KO* cells, which argue that regulation of this gene could occur at either translation, or mRNA stability, or both steps. Notably, *CHD8*, *SMC3* and *FAT1* are autism risk genes (41). Among the DEGs by Ribo-seq, we identified 42 autism risk genes and 33 schizophrenia risk genes (Table S4), supporting the hypothesis that TOP3B can regulate translation of genes important for mental disorders (2,3).

We used two methods, polysome profiling coupled with RT-qPCR and immunoblotting(42), to verify the Ribo-seq data that *CHD8* mRNA translation is reduced. Polysome profiling showed that the peak of *CHD8* mRNA in the heavy polysome fractions of *TOP3B-KO* cells was decreased, whereas that in the light polysome fractions was increased, in comparison to that of WT cells (Figure 3A), consistent with the Ribo-seq data that its translation was reduced. As controls, the level of *TOP3B* mRNA (positive control) was also decreased in the polysome fractions but increased in the monosomes in *TOP3B-KO* cells; and the level of *GAPDH* mRNA (negative control) was largely unchanged (Figure 3A). Immunoblotting further confirmed reduced CHD8 protein level in *TOP3B-KO* cells, whereas that of a control protein, GAPDH, was unchanged (Figure 3B). Together, these data indicate that the translation of *CHD8* mRNA is reduced when TOP3B is inactivated.

We noticed that there was a slight (20%~30%) and insignificant ($p>0.05$) reduction of *CHD8* mRNA level by RNA-seq (Figure 2C-D). RT-qPCR, which is more quantitative than RNA-seq, confirmed this reduction (about 30%), and also found it to be statistically significant ($p<0.05$) (Figure 3D). This reduction should not be caused by decreased transcription, because the nascent transcript level of *CHD8* in *TOP3B-KO* cells was found to be unchanged by PRO-seq (Figure 2D), and by RT-qPCR (Figure 3C). As a positive control, a gene regulated by TOP3B in transcription based on PRO-seq (Table S1), *ANXA10,* showed reduced nascent RNA level by RT-qPCR (Figure 3C). As a negative control, *TOP3B*, showed no change in nascent RNA by PRO-seq and RT-qPCR in *TOP3B-KO* cells (Table S1; Figure 3C).

To study whether the reduction of *CHD8* mRNA level is due to reduced translation, we pre-treated cells with a translational elongation inhibitor, cycloheximide (CHX), which is expected to increase the levels of those mRNAs subject to translation-associated mRNA decay (43). The *CHD8* mRNA in *TOP3B-KO*, but not *WT* cells, was significantly increased by CHX treatment (Figure 3D), indicating that the reduced level of the mRNA is due to reduced translation caused by the absence of TOP3B. As a positive control, *TOP3B* mRNA level was also increased by CHX treatment in *TOP3B-KO1* but not *WT* cells (Figure 3D). This is expected because the *TOP3B* frameshift mutations in *KO1* cells create premature stop codons in the earlier exons, making this mRNA a substrate of nonsense-mediated mRNA decay (NMD) that can be stabilized by inhibiting translation elongation (43). As another control, CHX treatment did not affect the mRNA level of *GAPDH*. In summary, these data suggest that TOP3B regulates translation of *CHD8* mRNA, and this process also stabilizes the mRNA. As a result, TOP3B inactivation reduces both translation and stability of *CHD8* mRNA.

TOP3B requires its topoisomerase activity to regulate translation and mRNA levels

We analyzed the data from *Y336F-KI* cell line to study whether TOP3B depends on its topoisomerase activity to function. The RNA-seq and Ribo-seq signals of *Y336F-KI* cells strongly correlated with those of *WT* cells (Figure S3D; R=0.95), which resemble those of *TOP3B-KO* cells (Figure S3A), suggesting that inactivating either TOP3B topoisomerase activity or the entire protein does not affect global mRNA levels or translation. Our RNA-seq and Ribo-seq analyses identified 1737 and 488 DEGs, separately, in *Y336F-KI* cells (Figure 4A; Table S2). Comparison of these DEGs with those of *TOP3B-KO* cells revealed the percentages of commonly decreased and increased DEGs: 21% and 42%, respectively by RNA-seq; and 12% and 13%, respectively by Ribo-seq (Figure 4B-D; Table S5). We then assessed whether the common DEGs of *Y336F-KI* cells showed the same direction of alteration in *TOP3B-KO* cells by chance using identical numbers of randomly selected and expression level-matched genes as comparisons. We found that the observed percentages of the commonly decreased or increased DEGs are about 6 to 10 -fold greater than those of the randomly selected genes (Figure 4B; Table S5), implying that the commonly altered DEGs are unlikely to occur by chance, but are most likely co-regulated by TOP3B and its catalytic activity. We refer to these genes as the TOP3B-Catalytic-Activity-dependent Genes (marked as "+" in Figure 4C-D). Conversely, the percentages of DEGs that are altered in opposite directions between *TOP3B-KO* and *Y336F-KI* cells are 3-10-fold lower than those of DEGs that are altered in the same direction, and are more similar to those of randomly selected genes (Figure 4B), indicating that TOP3B protein and its catalytic activity usually function in the same direction.

Our heatmap showed that a large fraction (about 58-88%) of the decreased or increased DEGs by RNA-seq or Ribo-seq in *TOP3B-KO* cells did not overlap with those in *Y336F-KI* cells (Figure 4C-D), suggesting that TOP3B may also regulate translation and RNA levels using mechanisms independent of its topoisomerase activity. Similarly, a large fraction (about 90%) of DEGs in *Y336F-KI* cells do not overlap with those of *TOP3B-KO* cells, hinting that the *TOP3B-Y336F* mutant protein may alter mRNA levels and translation in ways that are different from that caused by loss of the protein.

We examined the four representative genes that are altered in *TOP3B-KO* cells (Figure 2C), and found that three of them (*CHD8*, *EML3* and *FAT1*) exhibit the same direction of alteration in *Y336F-KI* cells: decreased or increased by Ribo-seq and RNA-seq analyses, and unchanged in PRO-seq analyses (Figure 5A-B), indicating that TOP3B topoisomerase activity is needed for normal translation and mRNA level control of these genes. This conclusion is further supported by immunoblotting, showing the same direction of alteration of CHD8 and FAT1 proteins between *TOP3B -KO* and *Y336F-KI* cells (Figure 3B & Figure S4A). Notably, the reduction of *CHD*8 mRNA in *Y336F-KI* cells was rescued by inhibiting translation with CHX treatment (Figure 3E), which is identical to the findings from *TOP3B-KO* cells in the same assay (Figure 3D), suggesting that the reduced *CHD8* mRNA levels in both *TOP3B-KO* and *Y336F-KI* cells are caused by reduced mRNA translation. Together, these data showed that some of the mRNAs regulated by TOP3B at translation level are topoisomerase activity dependent.

TOP3B co-regulates translation and mRNA levels with TDRD3 and FMRP

We studied whether TOP3B and its two partners, TDRD3 and FMRP, co-regulate a common set of genes. We analyzed *TDRD3-KO* and *FMR1-KO* cells using the same methods described above. The levels of RNA-seq and Ribo-seq of the two *KO* cells strongly correlated with those of *WT* cells (R>0.95; Figure S3E-F; Table S2). These features resemble those of *TOP3B-KO* cells, suggesting that inactivation of TOP3B-TDRD3 and FMRP affects neither global mRNA levels nor translation. Volcano plots identified about 1000~1500 DEGs in *TDRD3-KO* cells by each assay; and about 58~161 in *FMR1-KO* cells (Figure 6A). The number of DEGs in *TDRD3-KO* cells is about twice those of *TOP3B-KO* (Figure 6A and Figure 2A), consistent with the earlier data that TDRD3 can function independently of the TOP3B-TDRD3 complex (44).

Heatmaps revealed that the percentages of commonly downregulated (blue color) or upregulated (red color) DEGs between *TOP3B-KO* and *TDRD3-KO* are more than those between *TOP3B-KO* and *FMRP-KO* in both RNA-seq and Ribo-seq assays (Figure 6B-C; compare column 4 and 7). For example, the percentage of commonly decreased DEGs between *TOP3B-KO* and *TDRD3-KO* cells is about 3-fold higher than those between *TOP3B-KO* and *FMR1-KO* in RNA-seq (32% vs. 13%) and Ribo-seq (52% vs. 18%) (Figure 6B-C). The data suggest that TOP3B coregulates more genes with TDRD3 than with FMRP. The findings correlate with the interaction data that TOP3B forms a stoichiometric complex with TDRD3, and only a minor fraction of this complex interacts with FMRP (2,3,45).

We then assessed whether the observed percentages of common DEGs of *TOP3B-KO* cells showing the same alteration in *TDRD3-KO* or *FMR1-KO* cells could happen by chance, using randomly selected and expression level-matched genes as controls. The results showed that the observed percentages are 6 to 10-fold higher respectively, than those of randomly selected genes in *TDRD3-KO* or *FMR1-KO* cells, indicating that these concomitantly altered DEGs are most likely co-regulated by TOP3B and its two partners (Figure 6D-E). In contrast, the percentages of DEGs showing the opposite alterations between either *TOP3B-KO* and *TDRD3-KO*, or *TOP3B-KO* and *FMR1-KO cells,* are comparable to those of randomly selected genes (Figure 6D-E); and are also about 4-20-fold fewer than DEGs altered in the same direction, indicating that TOP3B and its two partners largely act in the same direction in mRNA level control and translation.

We examined the four representative genes with the same direction of alteration in *TOP3B-KO* and *Y336F-KI* mutant cells (Figure 5) and found that they all display the same alteration in *TDRD3-KO* cells, but not in *FMR1-KO* (Figure 7A-B). The data support the notion that TOP3B co-regulate with more genes with TDRD3 than FMRP. In particular, the levels of *CHD8* RNA-seq and Ribo-seq were found to be significantly reduced in *TDRD3-KO*, but not *FMR1-KO* cells (Figure 7A-B). In addition, the reduction of *CHD8* mRNA in *TDRD3-KO* cells was also confirmed by RT-qPCR (Figure 3E). Moreover, this reduction of *CHD8* mRNA was rescued by inhibiting translation with CHX treatment (Figure 3E). These data resemble the findings from *TOP3B-KO* and *Y336F-KI* cells (Figure 3D and Figure 3E), in which the reduced *CHD8*

mRNA levels were also restored by inhibiting translation. Together, these data suggest that the TOP3B-TDRD3 complex and its topoisomerase activity enhances translation of *CHD8* mRNA, and this process also stabilizes the same mRNA.

TOP3B-TDRD3 regulates mRNAs in both topoisomerase-dependent and independent mechanisms

We hypothesize that the co-regulated mRNAs in both *TOP3B-KO* and *TDRD3-KO* cells (Figure 8A-B & Table S6) are controlled by the entire TOP3B-TDRD3 complex and investigated how these mRNAs are regulated by the topoisomerase activity and FMRP. Comparing to *WT* cells, the percentage of decreased mRNAs is roughly equal to that of the increased mRNAs in RNA-seq (52% vs. 48%); and about 50% fewer (40% vs. 60%) in Ribo-seq (Figure 8A-B), suggesting that the TOP3B-TDRD3 complex can affect gene expression either positively or negatively. There is strong overlap between RNA-seq and Ribo-seq data in both *TOP3B-KO* and *TDRD3-KO* cells: 60%-78% for the decreased DEGs, and 52%-94% for increased DEGs, suggesting a coordinated regulation by TOP3B-TDRD3 (Figure 8A-B, columns 2, 5). To determine whether the complex acts transcriptionally or post-transcriptionally, we analyzed PRO-seq levels for these DEGs. Only about 20~30% of these DEGs exhibit concomitant changes in PRO-seq levels (Figure 8A-B, columns 3,6), which suggests that the TOP3B-TDRD3 complex mainly regulates gene expression post-transcriptionally.

We found that about 30%~40% of the decreased DEGs from both TOP3B and TDRD3-KO cells were concomitantly decreased in *Y336F-KI* cells, whereas about 20~30% were decreased in *FMR1-KO* cells (Figure 8A-B, column 7 and 10). The data thus suggest that some but not all mRNAs regulated by the TOP3B-TDRD3 complex are under the control of the topoisomerase activity of TOP3B and FMRP.

The mRNAs altered in both *TOP3B-KO* and *TDRD3-KO* cells include 29 mental disorder-related genes (Figure 8C). Eleven of them were also reduced in *Y336F-KI* cells (Figure 8C). Two representative transcripts (*CHD8* and *FAT1*) exhibited the same direction of alteration of Ribo-seq signals in *TOP3B-KO*, *TDRD3-KO*, and *Y336F-KI* cells (Figure 2C and 5C). Conversely, four other representative transcripts (*PRR12*, *SBF1, SATB2* and *BCORL1*) showed the same direction of alteration of Ribo-seq signals in *TOP3B-KO* and *TDRD3-KO* cells, but not *Y336F-KI* cells (Figure 8D). These findings reinforce the notion that the TOP3B-TDRD3 complex can regulate the expression of genes important for mental disorders in topoisomerase activity dependent and independent manners.

TOP3B preferentially binds long mRNAs enriched in mental disorder genes

We performed eCLIP-seq to identify TOP3B-bound mRNAs in *WT* HCT116 cells using a TOP3B antibody (34). To exclude the nonspecific signals due to antibody cross reactivity, we included a mock eCLIP-seq in TOP3B-KO cells as a negative control. After subtraction of the signals from the negative control, we identified 1106 TOP3B-bound mRNAs based on two independent experiments in HCT116 cells (Table S7).

These include several representative mRNAs described above: *CHD8*, *EML3* and *FAT1* (Figure 2C). BedGraph analysis confirmed the presence of TOP3B peaks that are higher in *WT* than *TOP3B-KO* cells (Figure 2C), suggesting that TOP3B can specifically binds these mRNAs. As negative controls, bedGraphs also confirmed the eCLIP-seq data that TOP3B signals are not reduced in *GAPDH* and *SMC3* mRNAs in *Top3B-KO* cells.

We verified the eCLIP-seq data by performing RNA immunoprecipitation (RIP) RT-qPCR (46) for four representative mRNAs: two positive (*CHD8* and *FAT1*), and two negative hits (*ACTB* and *GAPDH*). (Figure S5C). Consistent with the eCLIP data, the TOP3B antibody co-immunoprecipitated with *CHD8* and *FAT1* mRNAs, but not *ACTB* and *GAPDH* mRNAs (Figure S5C). As a control, TOP3B antibody immunoprecipitated TOP3B protein, but not beta-actin (Figure S5C). Together, our data are consistent our earlier findings based on HITS-CLIP that TOP3B can bind specific mRNAs and regulate their translation and mRNA levels (3).

Comparison between the current and old TOP3B-bound mRNAs revealed that about 1/3 of the mRNAs identified by eCLIP matched those identified from HeLa cells by HITS-CLIP(3) (Figure S5A). Those with higher eCLIP-seq signals tend to have higher HITS-CLIP signals (Figure 9A), suggesting that TOP3B may recognize specific features of these mRNAs. We found several features that are common in TOP3B-bound mRNAs identified in the current and previous studies, which are also shared by FMRP-bound mRNAs. First, the largest fraction of TOP3B CLIP-reads (~50%) are localized in coding regions of mRNAs (Figure 9B) (3), consistent with findings that TOP3B-TDRD3 associates with polyribosomes and regulates translation. Second, the average lengths of these mRNAs are significantly longer than that of randomly selected unbound mRNAs (Figure 9C) (3,47). This also resembles findings that TOP1 and TOP2-regulated genes that tend to have longer average lengths and are enriched in genes important for autism and neurological disorders (48). Third, a fraction of TOP3B-bound mRNAs (17%) from both current and previous studies overlapped with those bound by FMRP (Figure S5B) (49), including many autism (https://gene.sfari.org/), and schizophrenia-related (http://bioinfo.mc.vanderbilt.edu/SZGR/) mRNAs (109 and 59, respectively) (Figure 9D; Table S7), supporting the proposal that TOP3B may work with FMRP to regulate translation of mRNAs important for mental disorders (3).

TOP3B mRNA binding but not its topoisomerase activity stabilizes target mRNAs

We next examined the effects of TOP3B inactivation on its bound mRNAs in RNA-seq or Ribo-seq analyses. In both cases, the levels of RNA and RPFs in *TOP3B-KO* cells strongly correlate with those of *WT* cells (Figure 9H); and a minor fraction of TOP3B-bound mRNAs (5% or less; 58 out of 1106) displayed altered RNA-seq levels in *TOP3B-KO* cells (Figure 9E; Table S8). Interestingly, among those with altered mRNA levels, almost all of them (57 of 58) were decreased, whereas only one mRNA (*FAT1*) was increased (Figure 9E). In contrast, only 9% of these decreased DEGs showed this trend by PRO-seq analysis (Figure 10A), indicating that this decrease in RNA-seq signals is not due to reduced transcription. In support of this

notion, TOP3B-bound mRNAs exhibited overall reduced RNA-seq signals in *TOP3B-KO* cells than *WT* cells (Figure 9G; Figure 9H, left panel, more genes are below the equal line). As a control, TOP3B-bound mRNAs did not exhibit overall reduction in their nascent RNAs as determined by PRO-seq in *TOP3B-KO* cells (Figure 9H, right panel), indicating that TOP3B regulating its bound mRNAs post-transcriptionally. Because mRNA stabilization is a common feature of RNA binding proteins (RBPs) (50), our data suggest that Top3B likely stabilizes its bound mRNAs as an RBP.

In support of this suggestion, analysis of the TOP3B-bound mRNAs in *Y336F-KI* cells did not reveal a similar overall decrease (Figure S5D left, the number of the decrease vs. increased genes: 48 vs. 63). Moreover, only 18% of the Top3B-bound mRNAs showing reduced RNA-seq signals in Top3B-KO cells exhibited the same reduction in Y336F-KI cells. These data suggest that stabilization of Top3B-bound mRNAs is largely independent of the topoisomerase activity. As examples, two representative mRNAs, *AGRN* and *KIAA0100*, were found to be bound by TOP3B; and their RNA-seq, but not PRO-seq, signals were significantly reduced in both *TOP3B-KO* and *TDRD3-KO*, but not in *Y336F-KI* cells (Figure 10C-D), indicating that they are stabilized by TOP3B-TDRD3 binding but not topoisomerase activity.

Our analysis of TOP3B-bound mRNAs in Ribo-seq found that the numbers of mRNAs showing decreased or increased signals are comparable (33 vs. 44) (Figure 9F and 10B), suggesting that TOP3B binding may either enhance or suppress translation of its target mRNAs. Notably, more than half of them (56%) also showed the same trends in *TDRD3-KO* cells, whereas only 10% showed this trend in *FMRP-KO* cells, indicating that majority of these mRNAs are co-regulated by TDRD3, but a very small fraction are co-regulated with FMRP (Figure 10B). In addition, about 20% ~ 40% of them display the same trends in *Y336F-KI* cells (Figure 10B), suggesting that TOP3B topoisomerase activity is required for normal translation of a small fraction of mRNAs.

DISCUSSION

One challenging question for the topoisomerase field is whether mRNA metabolism produces topological stress that depends on a topoisomerase to solve. TOP3B has been suggested to work with TDRD3 and FMRP to regulate mRNA translation (3,6,7,9), but direct evidence supporting this suggestion is lacking. It is also unclear whether TOP3B depends on its topoisomerase activity to function on mRNA. Here we analyzed mRNA translation and abundance in newly established HCT116 cells individually inactivated of TOP3B, TOP3B catalytic activity, and its two partners; and obtained evidence that TOP3B-TDRD3 can regulate mRNA translation and abundance in topoisomerase activity-dependent and independent manners.

TOP3B cooperates with TDRD3 and FMRP to regulate mRNA translation and abundance

TOP3B and TDRD3 have been shown to form a stochiometric complex, but whether the two proteins work cooperatively or antagonistically remains unclear. We reasoned that if the two proteins act cooperatively,

inactivating each protein should alter mRNA translation and levels in the same direction. If they act antagonistically, inactivating each protein could alter mRNA in opposite directions. Comparison of RNA-seq and Ribo-seq data between *TOP3B-KO* and TDRD3-KO cells revealed that the fractions of overlapping mRNAs showing the same directions of alteration are 10-20 fold higher than those showing the opposite directions (Figure 6D). Moreover, the observed percentages of the overlapping mRNA showing the same directions of alteration are 6-10 fold higher than the predicted percentages if the overlap would occur by chance (Figure 6D). This is in contrast to the observed percentages of the mRNAs showing the opposite directions of alteration, which are similar or lower than the predicted percentages if the overlap would occur by chance. The data suggest that TOP3B and TDRD3 act cooperatively to regulate mRNA translation and abundance. The data are consistent with earlier findings that TDRD3 can stimulate the topoisomerase activity of TOP3B (51), and that the two proteins stabilize each other (7).

TOP3B-TDRD3 has also been suggested to interact with FMRP to regulate mRNA translation (2,3), but whether they work cooperatively or antagonistically is also unknown. Our analysis of RNA-seq and Ribo-seq data from *TOP3B-KO* and *FMRP-KO* data revealed a similar pattern as that between *TOP3B-KO* and *TDRD3-KO* cells: the overlapping mRNAs with the same directions of alterations are 6-20 fold higher than those with the opposite directions (Figure 6E); and the observed percentages of former mRNAs far exceed the predicted percentages if the overlap would occur by chance, whereas those of the latter mRNAs are similar to the predicted percentages if the overlap would occur by chance. These data suggest that TOP3B-TDRD3 also cooperatively work with FMRP to regulate mRNA translation and abundance.

TOP3B preferentially binds long mRNAs and enhance their levels post-transcriptionally

We identified about 1100 TOP3B-bound mRNAs in HCT116 cells by eCLIP and found that they have common features to the previously identified TOP3B-bound mRNAs from HeLa cells, including: enrichment in coding regions, and preferentially binding to longer mRNAs. This latter feature resembles that of TOP1 and TOP2, which preferentially regulates longer genes (48). Perhaps, longer mRNAs may resemble longer DNA in producing more topological barriers, which depend on topoisomerases to solve. It should be mentioned that longer genes tend to encode proteins important for neuronal function and mental disorders (48). Our data thus imply that TOP3B inactivation may disrupt translation or abundance of longer mRNAs encoding proteins important for mental disorders, which could contribute to increased disease risk in its mutant carriers.

Interestingly, we found that the most obvious effect of TOP3B inactivation on its bound mRNAs is their abundance. For example, for mRNAs that are altered in *TOP3B-KO* cells by RNA-seq, the percentage of decreased vs. increased mRNAs is 61% vs. 39% (Figure 6B). However, for TOP3B-bound mRNAs, the percentage of decreased vs. increased becomes about 99% vs. 1% (Figure 10A). In contrast, for mRNAs that are altered in TOP3B by Ribo-seq, the ratio between the decreased vs. increased in total mRNA, 42% vs. 58%, is nearly identical to that of TOP3B-bound mRNA (43% vs. 57%). The data suggest that the

TOP3B binding mainly enhances the levels of its bound mRNAs, but not their translation. It is intriguing that TOP3B bound mRNAs did not show a drastic alteration in translation when compared to the total mRNA. One possibility is that when TOP3B binds an mRNA, it may not necessarily catalyze topological reactions on this mRNA. It is known that for TOP1 and TOP2, their DNA targets identified by ChIP-seq are often different from those identified by methods that are based on capturing the intermediate of topoisomerase reactions--DNA-topoisomerase cleavage complex (52-57). The targets identified by the latter methods more actually represent the genes that are catalytically regulated by the topoisomerases. Similar methods need to be developed in future to identify mRNAs that are catalytically regulated by TOP3B. We predict that such mRNAs will show an overall trend of alteration when compared to total mRNAs.

TOP3B functions in topoisomerase activity-dependent and independent mechanisms

How TOP3B binding increases the levels of its bound mRNAs? PRO-seq data revealed that for TOP3b-bound mRNAs showing reduced mRNA levels in *TOP3B-KO* cells, most of them (about 90%) do not show reduced nascent RNA levels, indicating that TOP3B uses post-transcriptional mechanisms in this process. It is known that many RBPs can stabilize their bound mRNAs (50). In fact, the FMRP-bound mRNAs show reduced levels in its KO cells (37), which resemble our findings of TOP3B-bound mRNAs. TOP3B possesses not only RNA topoisomerase activity, but also mRNA-binding activity which strongly depends on its RNA-binding domain (RGG-box) (3,9). We propose that TOP3B may increase the levels of its bound mRNA by stabilizing them through mechanisms similar to those used by other RBPs. In support of this proposal, majority of TOP3B-bound mRNAs (about 80%) that show reduced levels in *TOP3B-KO* cells do not show significant reduction in *Y336F-KI* cells (Figure 10A and Figure S5D), suggesting that the mechanisms by which TOP3B stabilizes its bound mRNAs is topoisomerase activity-independent.

The findings that a topoisomerase can function independent of its enzymatic activity has precedence (58). We propose two mechanisms for how TOP3B may act in topoisomerase independent manners to regulate mRNA abundance and translation. One, in mRNA stabilization, TOP3B-TDRD3 complex may simply protect mRNAs from nuclease attacks, or otherwise assemble the mRNAs into a higher order complex that is more stable (Figure 11A). Two, in mRNA translation, TOP3B-TDRD3 may bind mRNAs through the RNA-binding domain of TOP3B, and recruit translation factors, including FMRP and EJC, through the Tudor and CTD domains of TDRD3 (2,3). FMRP may repress, whereas EJC may enhance, the first round of translation (Figure 11A-B).

Our Ribo-seq data revealed that some of TOP3B-bound mRNAs, such as *CHD8* mRNA, exhibit reduced translation in both *TOP3B-KO* and *Y336F-KI* cells. The reduced translation for *CHD8* mRNA was confirmed by polysome profiling and immunoblotting. Moreover, we show that the level of *CHD8* mRNA was reduced in both *KO* and *KI* cells of TOP3B, but this reduction is due to reduced translation of *CHD8* mRNA, because inhibiting translation elongation can restore the levels of *CHD8* mRNA of *TOP3B-KO, TDRD3-KO* and *KI* cells relative to the untreated cells. These data provide direct evidence that TOP3B can

bind and regulate translation of specific mRNA in topoisomerase activity-dependent mechanism. They also support our earlier model that mRNA translation may produce topological problems that depend on a topoisomerase to solve (Figure 11C-D).

The mRNA regulation by TOP3B is relevant to mental disorders and anti-viral studies

We have shown that the regulation of *CHD8* by TOP3B-TDRD3 complex is not at transcription, but at the post-transcriptional levels, because the nascent RNA levels of *CHD8* remain unchanged in *TOP3B-KO*, *Y336F-KI*, and *TDRD3-KO* cells, whereas those of CHD8 Ribo-seq and protein are reduced. Interestingly, *CHD8* mutations have been associated with autism in both human and mouse models (59,60). We found that in addition to CHD8, multiple genes related to autism or schizophrenia are bound and regulated by the TOP3B-TDRD3 in mRNA translation and/or abundance, but not in transcription, which support the notion that *TOP3B* mutations can contribute to the pathogenesis of psychiatric disorders (2,15,16).

Our findings that TOP3B topoisomerase activity is needed for translation of some of its bound mRNAs imply that TOP3B can form covalent cleavage complexes on RNA in cells, which is supported by a report that a self-cleavage mutant of TOP3B can form such complexes in cells (11). We propose that TOP3B-RNA cleavage complexes could be a target of anti-viral drugs. Because the resulting RNA damages consist of a protein-RNA crosslink and a strand break (Figure S6A-B), we expect that these damages should block viral RNA replication in a mechanism analogous to that employed by TOP1-DNA cleavage complex to block DNA replication. TOP3B has been proposed to be an anti-viral target, based on findings that its loss of function reduces viral RNA replication (12). Our proposal does not rely on the requirement of TOP3B for RNA viral replication, and postulates that as long as TOP3B can form cleavage complexes on viral RNAs, it should be a viable anti-viral target.

DATA AVAILABILITY

All next-generation sequencing data were deposited at GEO, and the accession number is GSE188574.

SUPPLEMENTARY DATA

Supplementary Data are available at NAR online.

FUNDING

Intramural Research Program of the National Institute on Aging, National Institutes of Health [Z01 AG000657-08 in part]; Intramural Research Program of the National Institute of Diabetes and Digestive and Kidney Disease, National Institutes of Health [ZO1 DK015602-09].

Conflict of interest statement. None declared.

ACKNOWLEDGEMENTS

We'd like to thank Dr. David Schlessinger for reading the manuscript and giving helpful advice. This work utilized the computational resources of the NIH HPC Biowulf Cluster and NIA computer servers.

REFERENCES:

1. Pommier, Y., Sun, Y., Huang, S.N. and Nitiss, J.L. (2016) Roles of eukaryotic topoisomerases in transcription, replication and genomic stability. *Nat Rev Mol Cell Biol*, **17**, 703-721.
2. Stoll, G., Pietilainen, O.P.H., Linder, B., Suvisaari, J., Brosi, C., Hennah, W., Leppa, V., Torniainen, M., Ripatti, S., Ala-Mello, S. *et al.* (2013) Deletion of TOP3beta, a component of FMRP-containing mRNPs, contributes to neurodevelopmental disorders. *Nat Neurosci*, **16**, 1228-1237.
3. Xu, D., Shen, W., Guo, R., Xue, Y., Peng, W., Sima, J., Yang, J., Sharov, A., Srikantan, S., Yang, J. *et al.* (2013) Top3beta is an RNA topoisomerase that works with fragile X syndrome protein to promote synapse formation. *Nat Neurosci*, **16**, 1238-1247.
4. Ahmad, M., Xu, D. and Wang, W. (2017) Type IA topoisomerases can be "magicians" for both DNA and RNA in all domains of life. *RNA Biol*, **14**, 854-864.
5. Ahmad, M., Xue, Y., Lee, S.K., Martindale, J.L., Shen, W., Li, W., Zou, S., Ciaramella, M., Debat, H., Nadal, M. *et al.* (2016) RNA topoisomerase is prevalent in all domains of life and associates with polyribosomes in animals. *Nucleic Acids Res*, **44**, 6335-6349.
6. Joo, Y., Xue, Y., Wang, Y., McDevitt, R.A., Sah, N., Bossi, S., Su, S., Lee, S.K., Peng, W., Xie, A. *et al.* (2020) Topoisomerase 3beta knockout mice show transcriptional and behavioural impairments associated with neurogenesis and synaptic plasticity. *Nat Commun*, **11**, 3143.
7. Yang, Y., McBride, K.M., Hensley, S., Lu, Y., Chedin, F. and Bedford, M.T. (2014) Arginine methylation facilitates the recruitment of TOP3B to chromatin to prevent R loop accumulation. *Mol Cell*, **53**, 484-497.
8. Zhang, T., Wallis, M., Petrovic, V., Challis, J., Kalitsis, P. and Hudson, D.F. (2019) Loss of TOP3B leads to increased R-loop formation and genome instability. *Open Biol*, **9**, 190222.
9. Ahmad, M., Shen, W., Li, W., Xue, Y., Zou, S., Xu, D. and Wang, W. (2017) Topoisomerase 3beta is the major topoisomerase for mRNAs and linked to neurodevelopment and mental dysfunction. *Nucleic Acids Res*, **45**, 2704-2713.
10. Lee, S.K., Xue, Y., Shen, W., Zhang, Y., Joo, Y., Ahmad, M., Chinen, M., Ding, Y., Ku, W.L., De, S. *et al.* (2018) Topoisomerase 3beta interacts with RNAi machinery to promote heterochromatin formation and transcriptional silencing in Drosophila. *Nat Commun*, **9**, 4946.
11. Saha, S., Sun, Y., Huang, S.N., Baechler, S.A., Pongor, L.S., Agama, K., Jo, U., Zhang, H., Tse-Dinh, Y.C. and Pommier, Y. (2020) DNA and RNA Cleavage Complexes and Repair Pathway for TOP3B RNA- and DNA-Protein Crosslinks. *Cell Rep*, **33**, 108569.
12. Prasanth, K.R., Hirano, M., Fagg, W.S., McAnarney, E.T., Shan, C., Xie, X., Hage, A., Pietzsch, C.A., Bukreyev, A., Rajsbaum, R. *et al.* (2020) Topoisomerase III-beta is required for efficient replication of positive-sense RNA viruses. *Antiviral Res*, **182**, 104874.
13. Kashima, I., Jonas, S., Jayachandran, U., Buchwald, G., Conti, E., Lupas, A.N. and Izaurralde, E. (2010) SMG6 interacts with the exon junction complex via two conserved

EJC-binding motifs (EBMs) required for nonsense-mediated mRNA decay. *Genes Dev*, **24**, 2440-2450.
14. Morettin, A., Paris, G., Bouzid, Y., Baldwin, R.M., Falls, T.J., Bell, J.C. and Cote, J. (2017) Tudor Domain Containing Protein 3 Promotes Tumorigenesis and Invasive Capacity of Breast Cancer Cells. *Scientific reports*, **7**, 5153.
15. Iossifov, I., Ronemus, M., Levy, D., Wang, Z., Hakker, I., Rosenbaum, J., Yamrom, B., Lee, Y.H., Narzisi, G., Leotta, A. *et al.* (2012) De novo gene disruptions in children on the autistic spectrum. *Neuron*, **74**, 285-299.
16. Xu, B., Ionita-Laza, I., Roos, J.L., Boone, B., Woodrick, S., Sun, Y., Levy, S., Gogos, J.A. and Karayiorgou, M. (2012) De novo gene mutations highlight patterns of genetic and neural complexity in schizophrenia. *Nat Genet*, **44**, 1365-1369.
17. Riley, J.D., Delahunty, C., Alsadah, A., Mazzola, S. and Astbury, C. (2020) Further evidence of GABRA4 and TOP3B as autism susceptibility genes. *Eur J Med Genet*, **63**, 103876.
18. Yu, T.W. and Berry-Kravis, E. (2014) Autism and fragile X syndrome. *Semin Neurol*, **34**, 258-265.
19. Ran, F.A., Hsu, P.D., Wright, J., Agarwala, V., Scott, D.A. and Zhang, F. (2013) Genome engineering using the CRISPR-Cas9 system. *Nat Protoc*, **8**, 2281-2308.
20. Ingolia, N.T., Brar, G.A., Rouskin, S., McGeachy, A.M. and Weissman, J.S. (2012) The ribosome profiling strategy for monitoring translation in vivo by deep sequencing of ribosome-protected mRNA fragments. *Nat Protoc*, **7**, 1534-1550.
21. Gerashchenko, M.V. and Gladyshev, V.N. (2017) Ribonuclease selection for ribosome profiling. *Nucleic Acids Res*, **45**, e6.
22. Van Nostrand, E.L., Nguyen, T.B., Gelboin-Burkhart, C., Wang, R., Blue, S.M., Pratt, G.A., Louie, A.L. and Yeo, G.W. (2017) Robust, Cost-Effective Profiling of RNA Binding Protein Targets with Single-end Enhanced Crosslinking and Immunoprecipitation (seCLIP). *Methods Mol Biol*, **1648**, 177-200.
23. Mahat, D.B., Kwak, H., Booth, G.T., Jonkers, I.H., Danko, C.G., Patel, R.K., Waters, C.T., Munson, K., Core, L.J. and Lis, J.T. (2016) Base-pair-resolution genome-wide mapping of active RNA polymerases using precision nuclear run-on (PRO-seq). *Nature Protocols*, **11**, 1455-1476.
24. Penalva, L.O., Tenenbaum, S.A. and Keene, J.D. (2004) Gene expression analysis of messenger RNP complexes. *Methods Mol Biol*, **257**, 125-134.
25. Chen, F.X., Marshall, S.A., Deng, Y. and Tianjiao, S. (2018) Measuring Nascent Transcripts by Nascent-seq. *Methods Mol Biol*, **1712**, 19-26.
26. Kim, D., Paggi, J.M., Park, C., Bennett, C. and Salzberg, S.L. (2019) Graph-based genome alignment and genotyping with HISAT2 and HISAT-genotype. *Nat Biotechnol*, **37**, 907-915.
27. Anders, S., Pyl, P.T. and Huber, W. (2015) HTSeq-a Python framework to work with high-throughput sequencing data. *Bioinformatics*, **31**, 166-169.
28. Love, M.I., Huber, W. and Anders, S. (2014) Moderated estimation of fold change and dispersion for RNA-seq data with DESeq2. *Genome Biology*, **15**.
29. Ramirez, F., Dundar, F., Diehl, S., Gruning, B.A. and Manke, T. (2014) deepTools: a flexible platform for exploring deep-sequencing data. *Nucleic Acids Research*, **42**, W187-W191.

30. Robinson, J.T., Thorvaldsdottir, H., Winckler, W., Guttman, M., Lander, E.S., Getz, G. and Mesirov, J.P. (2011) Integrative genomics viewer. *Nature Biotechnology*, **29**, 24-26.
31. Langmead, B. and Salzberg, S.L. (2012) Fast gapped-read alignment with Bowtie 2. *Nature Methods*, **9**, 357-U354.
32. Wang, L., Wang, S. and Li, W. (2012) RSeQC: quality control of RNA-seq experiments. *Bioinformatics*, **28**, 2184-2185.
33. Aravind, L., Leipe, D.D. and Koonin, E.V. (1998) Toprim--a conserved catalytic domain in type IA and II topoisomerases, DnaG-type primases, OLD family nucleases and RecR proteins. *Nucleic Acids Res*, **26**, 4205-4213.
34. Van Nostrand, E.L., Pratt, G.A., Shishkin, A.A., Gelboin-Burkhart, C., Fang, M.Y., Sundararaman, B., Blue, S.M., Nguyen, T.B., Surka, C., Elkins, K. *et al.* (2016) Robust transcriptome-wide discovery of RNA-binding protein binding sites with enhanced CLIP (eCLIP). *Nat Methods*, **13**, 508-514.
35. Piccirillo, C.A., Bjur, E., Topisirovic, I., Sonenberg, N. and Larsson, O. (2014) Translational control of immune responses: from transcripts to translatomes. *Nat Immunol*, **15**, 503-511.
36. Blevins, W.R., Tavella, T., Moro, S.G., Blasco-Moreno, B., Closa-Mosquera, A., Diez, J., Carey, L.B. and Alba, M.M. (2019) Extensive post-transcriptional buffering of gene expression in the response to severe oxidative stress in baker's yeast. *Sci Rep-Uk*, **9**.
37. Liu, B., Li, Y., Stackpole, E.E., Novak, A., Gao, Y., Zhao, Y., Zhao, X. and Richter, J.D. (2018) Regulatory discrimination of mRNAs by FMRP controls mouse adult neural stem cell differentiation. *Proc Natl Acad Sci U S A*, **115**, E11397-E11405.
38. Brogna, S. and Wen, J. (2009) Nonsense-mediated mRNA decay (NMD) mechanisms. *Nat Struct Mol Biol*, **16**, 107-113.
39. Harigaya, Y. and Parker, R. (2010) No-go decay: a quality control mechanism for RNA in translation. *Wiley Interdiscip Rev RNA*, **1**, 132-141.
40. Kurosaki, T., Popp, M.W. and Maquat, L.E. (2019) Quality and quantity control of gene expression by nonsense-mediated mRNA decay. *Nat Rev Mol Cell Biol*, **20**, 406-420.
41. Abrahams, B.S., Arking, D.E., Campbell, D.B., Mefford, H.C., Morrow, E.M., Weiss, L.A., Menashe, I., Wadkins, T., Banerjee-Basu, S. and Packer, A. (2013) SFARI Gene 2.0: a community-driven knowledgebase for the autism spectrum disorders (ASDs). *Mol Autism*, **4**, 36.
42. Piccirillo, C.A., Bjur, E., Topisirovic, I., Sonenberg, N. and Larsson, O. (2014) Translational control of immune responses: from transcripts to translatomes. *Nat Immunol*, **15**, 503-511.
43. Ishigaki, Y., Li, X.J., Serin, G. and Maquat, L.E. (2001) Evidence for a pioneer round of mRNA translation: mRNAs subject to nonsense-mediated decay in mammalian cells are bound by CBP80 and CBP20. *Cell*, **106**, 607-617.
44. Narayanan, N., Wang, Z.H., Li, L. and Yang, Y.Z. (2017) Arginine methylation of USP9X promotes its interaction with TDRD3 and its anti-apoptotic activities in breast cancer cells. *Cell Discov*, **3**.
45. Goto-Ito, S., Yamagata, A., Takahashi, T.S., Sato, Y. and Fukai, S. (2017) Structural basis of the interaction between Topoisomerase III beta and the TDRD3 auxiliary factor. *Sci Rep-Uk*, **7**.
46. Gilbert, C. and Svejstrup, J.Q. (2006) RNA immunoprecipitation for determining RNA-protein associations in vivo. *Curr Protoc Mol Biol*, **Chapter 27**, Unit 27 24.

47. Sawicka, K., Hale, C.R., Park, C.Y., Fak, J.J., Gresack, J.E., Van Driesche, S.J., Kang, J.J., Darnell, J.C. and Darnell, R.B. (2019) FMRP has a cell-type-specific role in CA1 pyramidal neurons to regulate autism-related transcripts and circadian memory. *Elife*, **8**.
48. King, I.F., Yandava, C.N., Mabb, A.M., Hsiao, J.S., Huang, H.S., Pearson, B.L., Calabrese, J.M., Starmer, J., Parker, J.S., Magnuson, T. *et al.* (2013) Topoisomerases facilitate transcription of long genes linked to autism. *Nature*, **501**, 58-62.
49. Darnell, J.C., Van Driesche, S.J., Zhang, C., Hung, K.Y., Mele, A., Fraser, C.E., Stone, E.F., Chen, C., Fak, J.J., Chi, S.W. *et al.* (2011) FMRP stalls ribosomal translocation on mRNAs linked to synaptic function and autism. *Cell*, **146**, 247-261.
50. Hentze, M.W., Castello, A., Schwarzl, T. and Preiss, T. (2018) A brave new world of RNA-binding proteins. *Nat Rev Mol Cell Biol*, **19**, 327-341.
51. Siaw, G.E., Liu, I.F., Lin, P.Y., Been, M.D. and Hsieh, T.S. (2016) DNA and RNA topoisomerase activities of Top3beta are promoted by mediator protein Tudor domain-containing protein 3. *Proc Natl Acad Sci U S A*, **113**, E5544-5551.
52. Tiwari, V.K., Burger, L., Nikoletopoulou, V., Deogracias, R., Thakurela, S., Wirbelauer, C., Kaut, J., Terranova, R., Hoerner, L., Mielke, C. *et al.* (2012) Target genes of Topoisomerase IIbeta regulate neuronal survival and are defined by their chromatin state. *Proc Natl Acad Sci U S A*, **109**, E934-943.
53. Manville, C.M., Smith, K., Sondka, Z., Rance, H., Cockell, S., Cowell, I.G., Lee, K.C., Morris, N.J., Padget, K., Jackson, G.H. *et al.* (2015) Genome-wide ChIP-seq analysis of human TOP2B occupancy in MCF7 breast cancer epithelial cells. *Biology open*, **4**, 1436-1447.
54. Baranello, L., Wojtowicz, D., Cui, K.R., Devaiah, B.N., Chung, H.J., Chan-Salis, K.Y., Guha, R., Wilson, K., Zhang, X.H., Zhang, H.L. *et al.* (2016) RNA Polymerase II Regulates Topoisomerase 1 Activity to Favor Efficient Transcription. *Cell*, **165**, 357-371.
55. Uuskula-Reimand, L., Hou, H.Y., Samavarchi-Tehrani, P., Rudan, M.V., Liang, M.G., Medina-Rivera, A., Mohammed, H., Schmidt, D., Schwalie, P., Young, E.J. *et al.* (2016) Topoisomerase II beta interacts with cohesin and CTCF at topological domain borders. *Genome Biology*, **17**.
56. Canela, A., Maman, Y., Jung, S., Wong, N., Callen, E., Day, A., Kieffer-Kwon, K.R., Pekowska, A., Zhang, H., Rao, S.S.P. *et al.* (2017) Genome Organization Drives Chromosome Fragility. *Cell*, **170**, 507-521 e518.
57. Das, S.K., Kuzin, V., Cameron, D.P., Sanford, S., Jha, R.K., Nie, Z., Rosello, M.T., Holewinski, R., Andresson, T., Wisniewski, J. *et al.* (2022) MYC assembles and stimulates topoisomerases 1 and 2 in a "topoisome". *Mol Cell*, **82**, 140-158 e112.
58. Merino, A., Madden, K.R., Lane, W.S., Champoux, J.J. and Reinberg, D. (1993) DNA Topoisomerase-I Is Involved in Both Repression and Activation of Transcription. *Nature*, **365**, 227-232.
59. Xu, Q., Liu, Y.Y., Wang, X., Tan, G.H., Li, H.P., Hulbert, S.W., Li, C.Y., Hu, C.C., Xiong, Z.Q., Xu, X. *et al.* (2018) Autism-associated CHD8 deficiency impairs axon development and migration of cortical neurons. *Mol Autism*, **9**, 65.
60. Platt, R.J., Zhou, Y., Slaymaker, I.M., Shetty, A.S., Weisbach, N.R., Kim, J.A., Sharma, J., Desai, M., Sood, S., Kempton, H.R. *et al.* (2017) Chd8 Mutation Leads to Autistic-like Behaviors and Impaired Striatal Circuits. *Cell Rep*, **19**, 335-350.

FIGURE LEGENDS

Figure 1. Creating *TOP3B-TDRD3 KO* and *KI* cell lines to study their function. (**A**) A schematic diagram displaying the experimental design procedure. (**B**, **C**) Immunoblotting gel images (left) and quantification (19) confirm the absence of TOP3B, TDRD3 and FMRP proteins in their respective HCT116 knockout (*KO*) cells generated by CRISPR-Cas9 gene targeting method (*19*). The level of TOP3B-Y336F (**C**) was about 50% of that of *WT* cells, suggesting that the catalytic reaction may help to stabilize the topoisomerase protein. For the bar charts, all the values are normalized to *WT* and log-transformed before *P*-value calculation. * = *P*-value < 0.05, ** = *P*-value < 0.01 (Student's t-test). (**D**) Genomic sequencing results show the T to A substitution in *TOP3B-Y336F-KI* cell line generated by CRISPR-Cas9.

Figure 2. TOP3B Inactivation alters translation and abundance of specific mRNAs. (**A**) Volcano plots showing the numbers of down-regulated or upregulated differentially expressed genes (DEGs) in *TOP3B-KO* by RNA-seq (up) or Ribo-seq (down) from five independent experiments. (**B**) A heatmap shows expression changes (in fold change) between *TOP3B-KO* vs. *WT* for the DEGs identified by Ribo-seq. The DEGs with decreased or increased signals were marked by blue and red, respectively. The DEGs were divided into eight groups based on their RPF, mRNA and PRO-seq levels as described in the main text. Several representative genes altered at post-transcriptional level are marked on the right. (**C**, **D**) BedGraphs (**C**), and their quantifications (**D**), show that four representative genes with altered RPF levels in *TOP3B-KO* cells. eCLIP-seq results show the binding of TOP3B to three of them. The RNA-seq and PRO-seq were included for comparison. *GAPDH* was included as a control. The black arrows above the bedGraphs mark the TOP3B eCLIP peaks that were higher in *WT* and lower in *TOP3B-KO* cells (a negative control), whereas those below mark the transcription direction. Blue and red arrows (below) mark the positions of translation start and stop codons separately. Blue and red arrows (middle) mark the decrease or increase of the expression level separately. The data in (**D**) were shown in normalized counts generated by DESeq2. * = adjust *P*-value < 0.1, ** = adjust *P*-value < 0.05, *** = adjust *P*-value < 0.01.

Figure 3. TOP3B regulates translation and levels of *CHD8* mRNA. (**A**) Graphs from polysome profiling analysis show the reduced translation of *CHD8* mRNA, as evidence by its decreased level in the heavy polysome fractions, and increased level in light polysome fractions. The relative distributions (%) of the mRNAs on the sucrose gradients were quantified by RT-qPCR analysis. *TOP3B* and *GAPDH* were used as controls. The translation of *TOP3B* mRNA was significantly reduced in *TOP3B-KO1* cells caused by pre-mature stop codon induced by CRISPR-Cas9 editing. No obvious difference of the translation was observed for *GAPDH* mRNA. The results were reproducible and one representative result was shown here. (**B**) Immunoblotting images (left) and quantification (19) show that CHD8 protein levels were reduced in *TOP3B* and *TDRD3* mutant cells, as indicated on top. For the bar graphs, all the values are normalized to *WT* and log-transformed before *P*-value calculation * = *P*-value < 0.05, ** = *P*-value < 0.01. (**C**) The nascent mRNA levels of representative genes were detected by RT-qPCR. The results showed that there was no significant

change for *TOP3B* gene, slightly increased for *CHD8* and significantly reduced for *ANXA10* gene, which were consistent with the PRO-seq results (Table S1). (**D**) RT-qPCR results showing the mRNA levels of the representative genes. Cycloheximide (CHX) treatment (100μg/mL) for 3 hours increased *TOP3B* and *CHD8* mRNA level in *TOP3B-KO* cells compared with non-treatment cells, indicating that the reduced mRNA levels were translation related. (**E**) RT-qPCR results showing *CHD8* mRNA level. Cycloheximide (CHX) treatment (100μg/mL) for 3 hours increased *CHD8* mRNA level in *Y336F-KI* or *TDRD3-KO* cells compared with non-treatment cells, indicating that the altered mRNA levels were translation related.

Figure 4. TOP3B regulates mRNAs in topoisomerase activity dependent and independent manners. (**A**) Volcano plots showing the number of DEGs in *TOP3B-Y336F* by RNA-seq (up) or Ribo-seq (down). (**B**) Graphs to compare the percentages of overlapped DEGs in the same or opposite direction of alteration between *TOP3B-Y336F* and *TOP3B-KO* groups vs. those randomly selected genes. The percentages were relative to the DEGs numbers of *TOP3B-KO* group. The randomly selected genes were expression level matched, and the numbers were identical to that of the decreased or increased DEGs of *TOP3B-Y336F cells*. Blue arrows represent reduced, whereas red arrows represent increased DEGs. Arrows in the same direction depicted DEGs that were altered in the same direction in *TOP3B-KO* and *Y336F* cells. (**C**, **D**) Heatmaps display the DEGs in *TOP3B-KO* which were overlapped with those of *Y336F* cells by RNA-seq (**C**) or Ribo-seq (**D**). The DEGs with decreased or increased signals (fold changes) were marked by blue and red, respectively. The overlapped DEGs that were altered in the same directions were marked as "+", whereas the others were marked as "-". The percentages of the overlapped or non-overlapped DEGs were shown on the right.

Figure 5. TOP3B requires its topoisomerase activity to regulate translation and mRNA levels of specific genes. (**A**) BedGraphs of sequencing read distributions, and bar graphs of quantification of these reads (**B**), show the Ribo-seq, RNA-seq and PRO-seq signals for five representative genes. The alteration of these genes in *TOP3B-KO* cells were described in Figure 2C. The bar graphs show the normalized counts from three biological replicates. *** = adjust *P*-value < 0.01.

Figure 6. TOP3B co-regulates more genes with TDRD3 than with FMRP. (**A**) Volcano plots showing the numbers of down-regulated or upregulated differentially expressed genes (DEGs) in *TDRD3-KO* and *FMR1-KO* by RNA-seq (blue) or Ribo-seq (orange) from three independent experiments. (**B**, **C**) Heatmaps showing the concomitantly decreased (blue color) or increased (red color) expression changes of the DEGs in *TOP3B-KO* vs. those of *TDRD3-KO* and *FMR1-KO* cells by RNA-seq (**B**) or Ribo-seq (**C**). The percentages below the maps were calculated by artificially setting the decreased or increased DEGs of *TOP3B-KO* cells as 100% (column 1). The percentages of the DEGs of *TDRD3-KO* or *FMR1-KO* cells that were altered in the same directions were shown in a table below the figure. The cutoff threshold for the

increased or decreased DEGs is 1.5-fold. Notably, a stronger co-clustering was observed between *TOP3B-KO* and *TDRD3-KO* than that between *TOP3B-KO* and *FMR1-KO* (column 4 vs. 7). (**D**) Graphs to compare the percentages of overlapping DEGs in the same or opposite direction of alteration vs. those randomly selected genes between *TOP3B-KO* and *TDRD3-KO* cells. The DEGs were identified by either RNA-seq (blue) or Ribo-seq (orange). The percentages were relative to the DEGs numbers of *TOP3B-KO* cells. The randomly selected genes were expression level matched, and the numbers were identical to that of the decreased or increased DEGs of *TDRD3-KO cells*. The percentages of these genes that were decreased or increased in RNA-seq or Ribo-seq of *TDRD3-KO* cells were then calculated. Blue arrows represented reduced, whereas red arrows represented increased DEGs. Arrows in the same direction depicted DEGs that were altered in the same direction in *TOP3B-KO* and *TDRD3-KO* cells. (**E**) The DEGs between *TOP3B-KO* and *FMR1-KO* were analyzed using the same method as (**D**).

Figure 7. Inactivation of TDRD3 but not FMRP alters specific mRNAs in the same direction as inactivation of Top3B (**A, B**) BedGraphs of sequencing read distributions (**A**), and bar graphs of quantification of these reads (**B**), show the Ribo-seq, mRNA and PRO-seq signals for five representative genes in *TDRD3-KO* and *FMR1-KO* cells. Black arrows below mark the transcription direction. Blue and red arrows (below) mark the positions of translation start and stop codons separately. Blue and red arrows (middle) mark the decrease or increase of the expression level separately. Notably, the alteration of CHD8, SMC3, EML3 and FAT1 in TDRD3-KO but not FMRP-KO cells are in the same directions as those in *TOP3B-KO* and *Y336F* cells (described in Figure 2C and Figure 5A). Normalized counts were generated by DESeq2. *** = adjust *P*-value < 0.01.

Figure 8. Multiple mental disorder risk genes are regulated by both TOP3B and TDRD3. (**A, B**) Heatmaps showing how the concomitantly decreased (blue color) or increased (red color) DEGs in both *TOP3B-KO* and *TDRD3-KO* cells were overlapped with the DEGs in *TOP3B-Y336F* and *FMR1-KO* cells by RNA-seq (**A**) or Ribo-seq (**B**). The percentages below the maps were calculated by artificially setting the decreased or increased DEGs of both *TOP3B-KO* and *TDRD3-KO* cells as 100% (column 1 and 4 of each graph). The percentages of the DEGs of *TOP3B-Y336F* or *FMR1-KO* cells that were altered in the same directions were shown in a table below the figure. The DEGs identified by different Seq methods from each cell type were included in the analysis. The cutoff threshold for the increased or decreased DEGs is 1.5-fold. Notably, a stronger co-clustering was observed between *TOP3B-KO*/*TDRD3-KO* and *TOP3B-Y336F* than that between *TOP3B-KO/TDRD3-KO* and *FMR1-KO* (column 7 vs. 10). In addition, a stronger co-clustering was also detected between the levels of RPF and RNA than with PRO-seq for each cell type. (**C**) A table showing the DEGs associated with autism or schizophrenia in both *TOP3B-KO* and *TDRD3-KO* HCT116 cells. (**D**) BedGraphs showing the expression levels of five representative genes with altered RPFs levels in both *TOP3B-KO* and *TDRD3-KO* cells, but not Y336F-KI cells, indicating that they were regulated in

TOP3B topoisomerase activity independent manner. Black arrows below mark the transcription direction. Blue and red arrows (middle) mark the decrease or increase of the expression levels separately.

Figure 9. eCLIP-seq reveals that TOP3B prefers to bind coding region of long mRNAs and its binding stabilizes these mRNAs. (**A**) A ranked plot shows that genes containing high frequency of TOP3B eCLIP-seq tags from HCT116 cells were enriched with TOP3B HITS-CLIP targets from our previous study in HeLa cells (3). (**B**) A pie chart displaying eCLIP-seq read density (tags/kb) distribution in CDS, 5'UTR, 3'UTR and introns. Reads from *WT* immunoprecipitation group were analyzed using RSeQC. (**C**) Box and Whisker plot showing longer average of lengths of mRNAs bound by TOP3B identified by eCLIP in HCT116, HITS-CLIP in HeLa, or those bound by FMRP identified by HITS-CLIP in mouse brains, when compared to the non-targets (3,49). The mRNA lengths were log-transformed. (**D**) Venn diagrams showing the overlapped gene numbers between TOP3B targets with those of SFARI autism genes or those of schizophrenia risk genes. (**E, F**) Volcano plots showing the expression changes of TOP3B targets by RNA-seq (**E**) or Ribo-seq (**F**). (**G**) A Box-Whisker plot showing that TOP3B eCLIP target mRNAs have lower mRNA levels in *TOP3B-KO* cells compared with *WT* cells. As a control, the randomly selected unbound mRNAs (also expression level matched) does not have this trend. These data suggest that TOP3B binding stabilizes mRNAs. *** , p-value < 0.01; n.s., no significant. (**H**) Scatter plots showing the strong correlations of RNA, RPFs or PRO-seq levels of TOP3B eCLIP targets between *WT* and *TOP3B-KO* cells. Notably, there are more mRNAs with reduced RNA levels in *TOP3B-KO* HCT116 cells, indicating that TOP3B binding stabilizes mRNAs.

Figure 10. TOP3B stabilizes its bound mRNAs by topoisomerase activity independent manner. (**A**, **B**) Heatmaps showing the expression changes of the TOP3B-bound mRNAs determined by RNA-seq (**A**) or Ribo-seq (**B**), in different *KO* and *KI* mutant cells indicated on the top. The percentages below the maps were calculated by artificially setting the decreased or increased DEGs of *TOP3B-KO* cells as 100% (column 1 of each graph). The percentages of these DEGs altered in the same directions in other *KO* or *KI* mutant cells were shown in a table below the figure. The DEGs identified by different Seq methods from each cell type were included in the analysis. The cutoff threshold for the increased or decreased DEGs is 1.5-fold. Notably, the percentage of decreased TOP3B-bound mRNAs was much higher than that of increased by RNA-seq (**A**), whereas about the two percentages by Ribo-seq were roughly equal (**B**). (**C**) BedGraphs showing two representative TOP3B eCLIP-seq target mRNAs. The mRNA levels were significantly reduced in *TOP3B-KO* and *TDRD3-KO* cells. And their transcription by PRO-seq did not show reduction, indicating their mRNA stability were regulated by TOP3B and TDRD3. However, their mRNA levels are not reduced in *Y336F-KI* cells, which indicates that they are regulated by topoisomerase activity independent manner. (**D**) The bar graphs show the normalized counts from three biological replicates for RNA-seq and two replicates for PRO-seq. All the values were normalized to *WT*. **= adjust *P*-value < 0.05, *** = adjust *P*-value < 0.01.

Figure 11. Models showing how the TOP3B-TDRD3 complex regulates translation and RNA stability. (**A**) As RNA binding proteins, for one thing, the TOP3B-TDRD3 complex may simply protect mRNAs from nuclease attacks or assembles the mRNAs into a higher order complex that is more stable. For another, the TOP3B-TDRD3 complex may interact with EJC complex to enhance translation and mRNA stability (2). (**B**) The TOP3B-TDRD3 complex may suppress translation by recruiting FMRP to its target mRNAs (2,3,13). (**C**) The TOP3B-TDRD3 complex may resolve (decatenate) two tangled mRNAs to promote their translation and stability. This model is supported by *in vitro* assays showing TOP3B can catalyze catenation of RNA circles (3,51). (**D**) An mRNA may become topologically constrained by circularization during translation. A supercoil or knot-like structure may be formed and required an RNA topoisomerase to release (3).

Figure 1. Creating *TOP3B-TDRD3 KO* and *KI* cell lines to study their function.

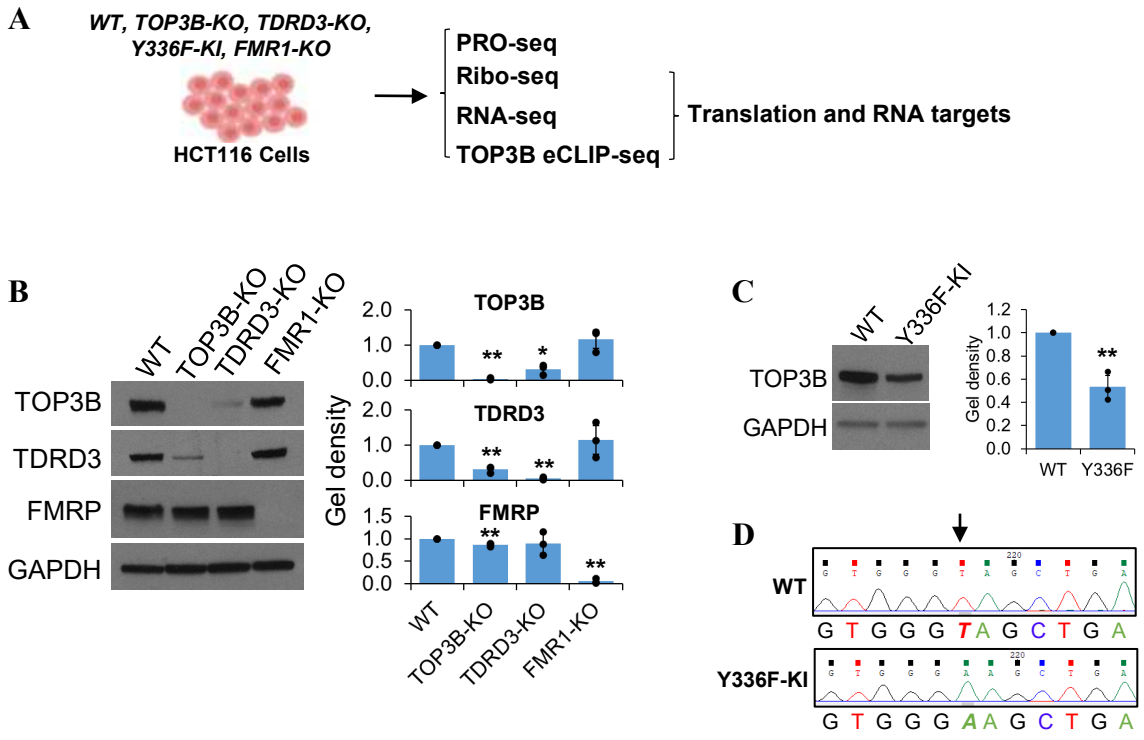

Figure 2. TOP3B inactivation alters translation and abundance of specific mRNAs

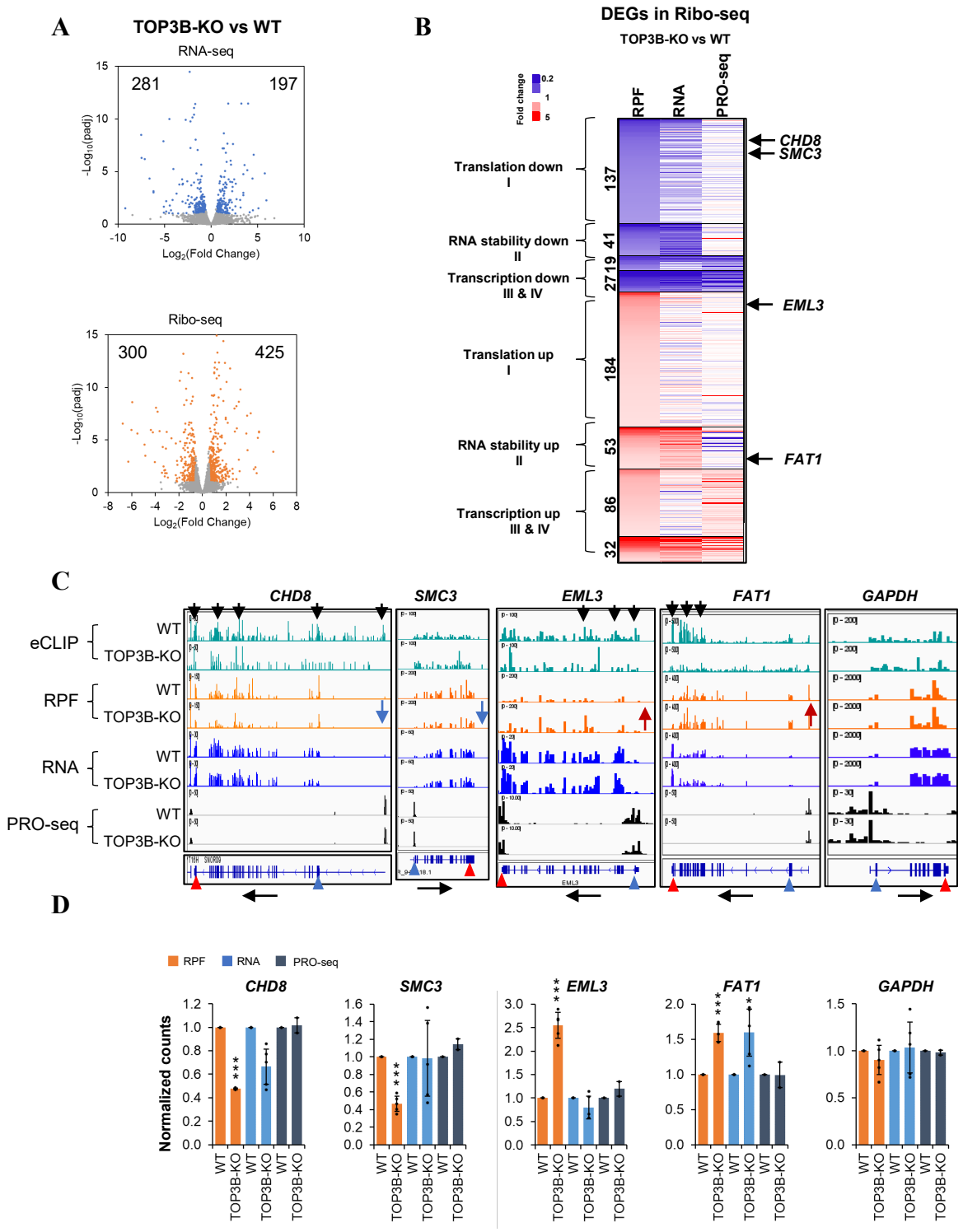

Figure 3. TOP3B regulates translation and levels of *CHD8* mRNA

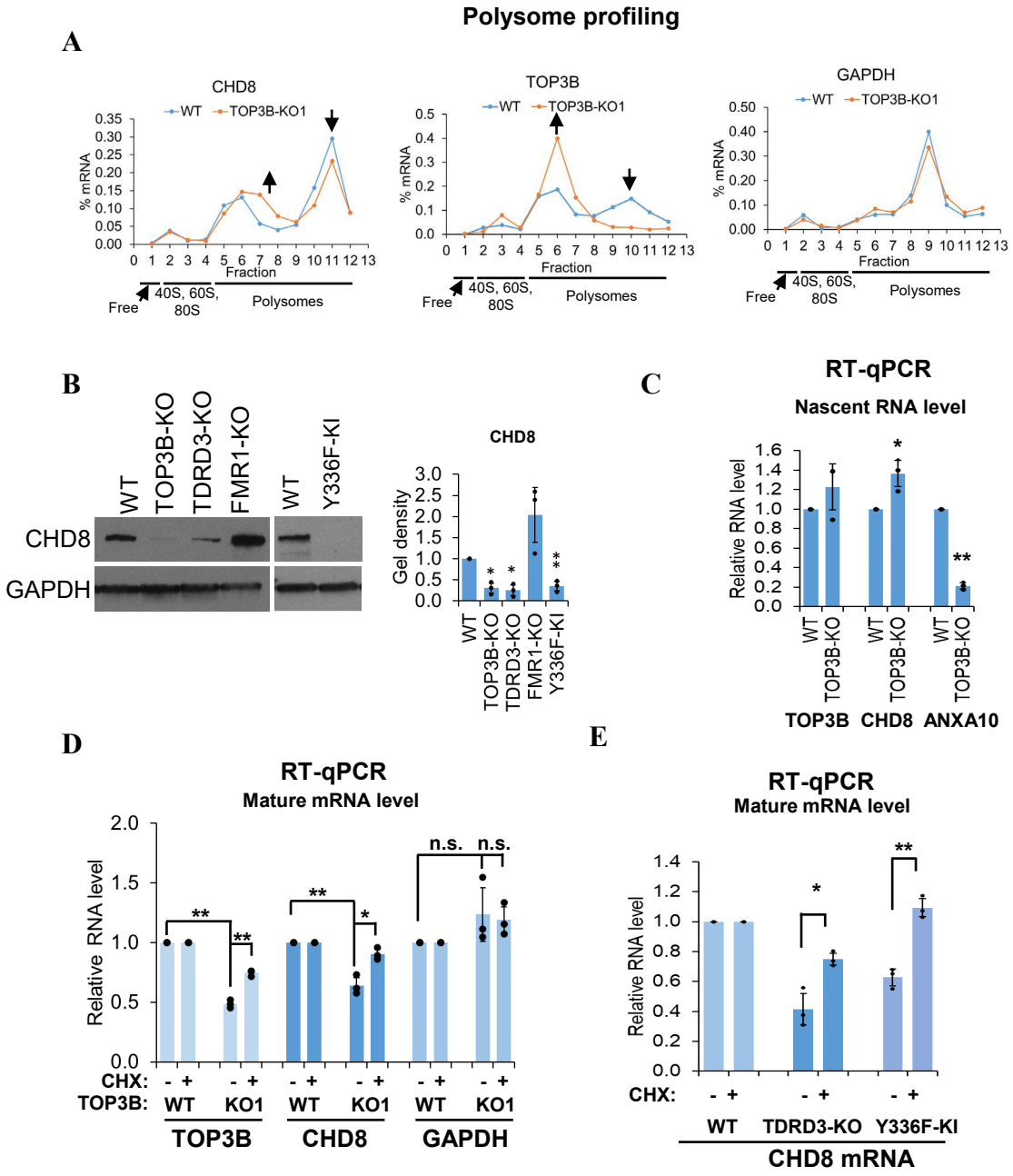

Figure 4. TOP3B regulates mRNAs in topoisomerase activity dependent and independent manners.

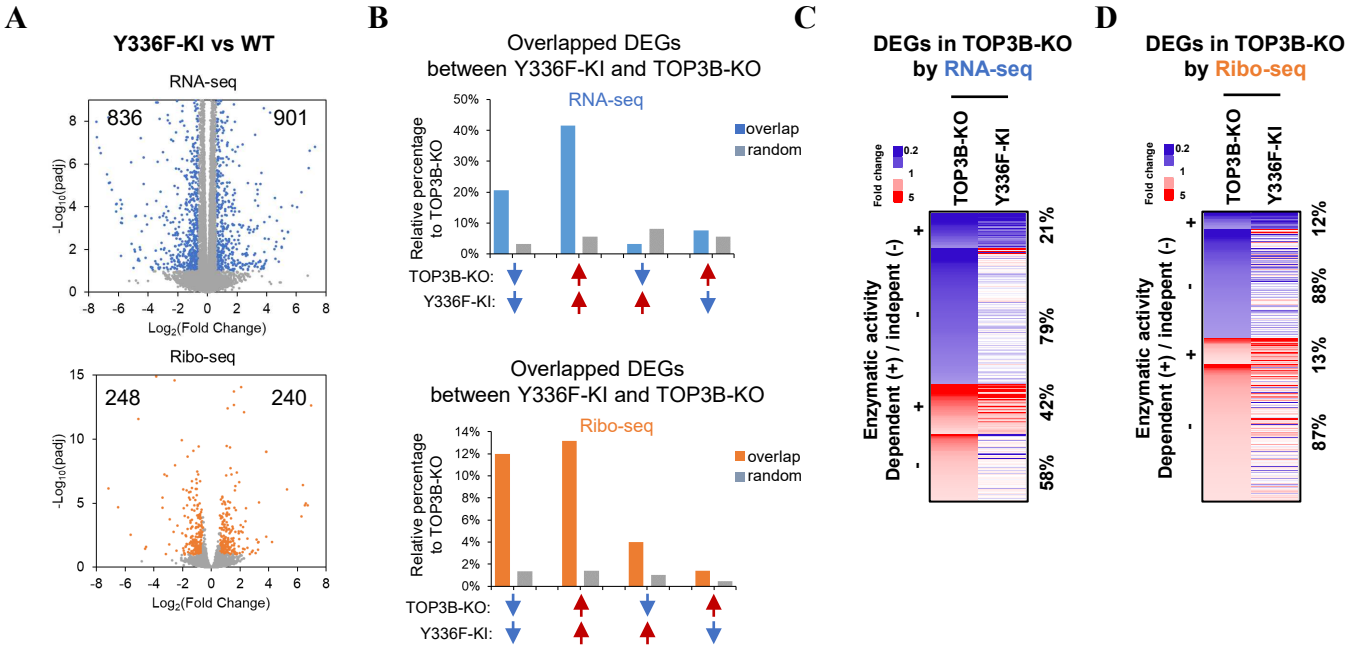

Figure 5. TOP3B requires its topoisomerase activity to regulate translation and mRNA levels of specific genes.

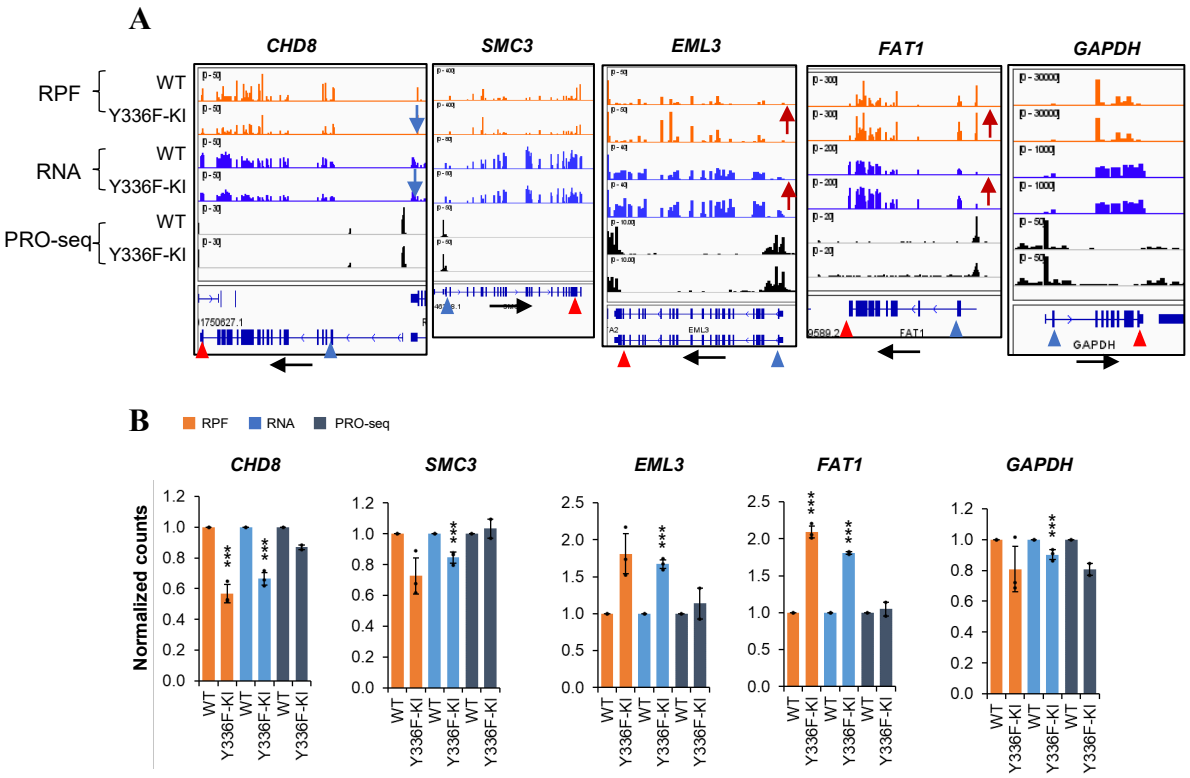

Figure 6. TOP3B co-regulates more genes with TDRD3 than with FMRP.

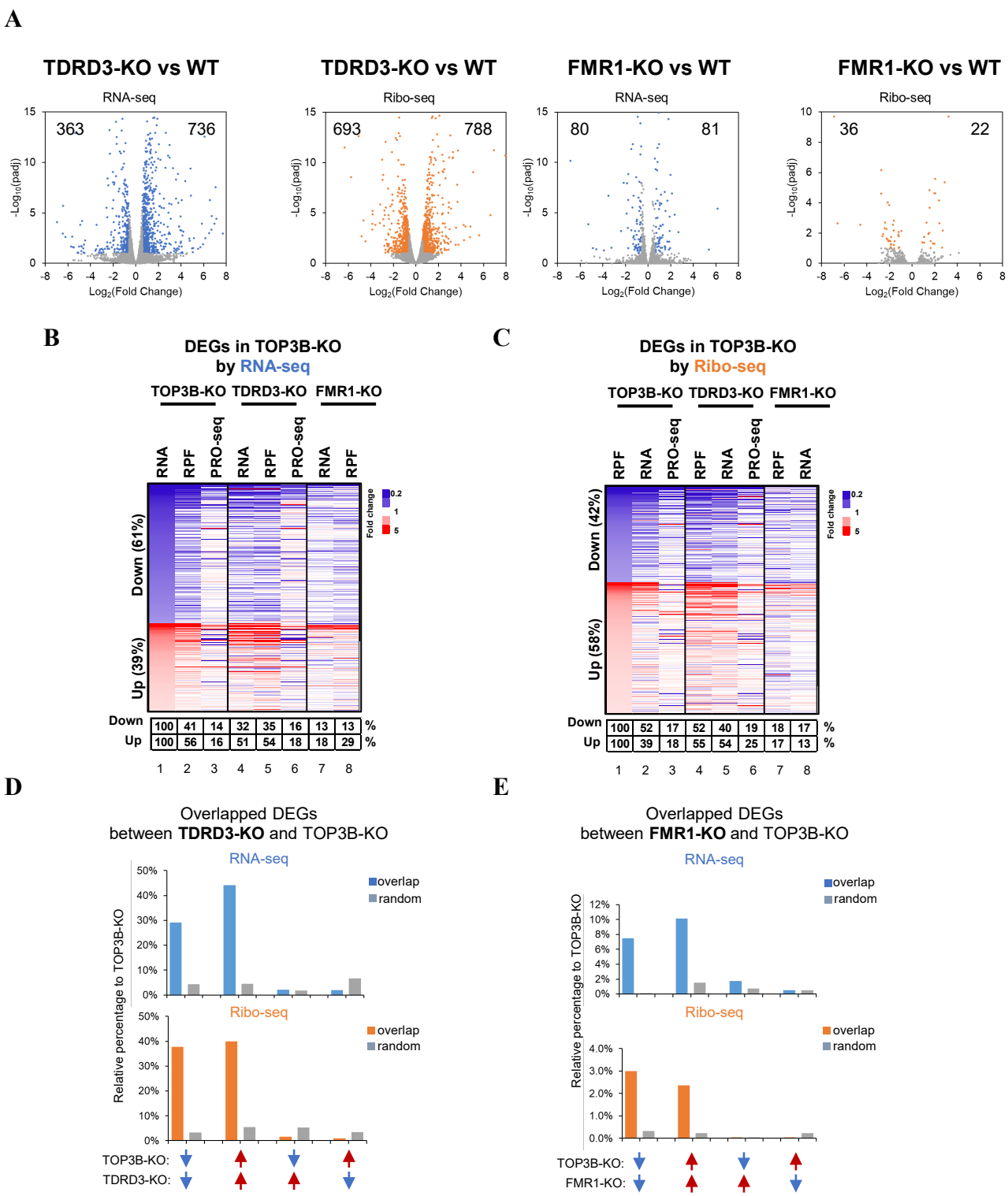

Figure 7. Inactivation of TDRD3 but not FMRP alters specific mRNAs in the same direction as inactivation of Top3B.

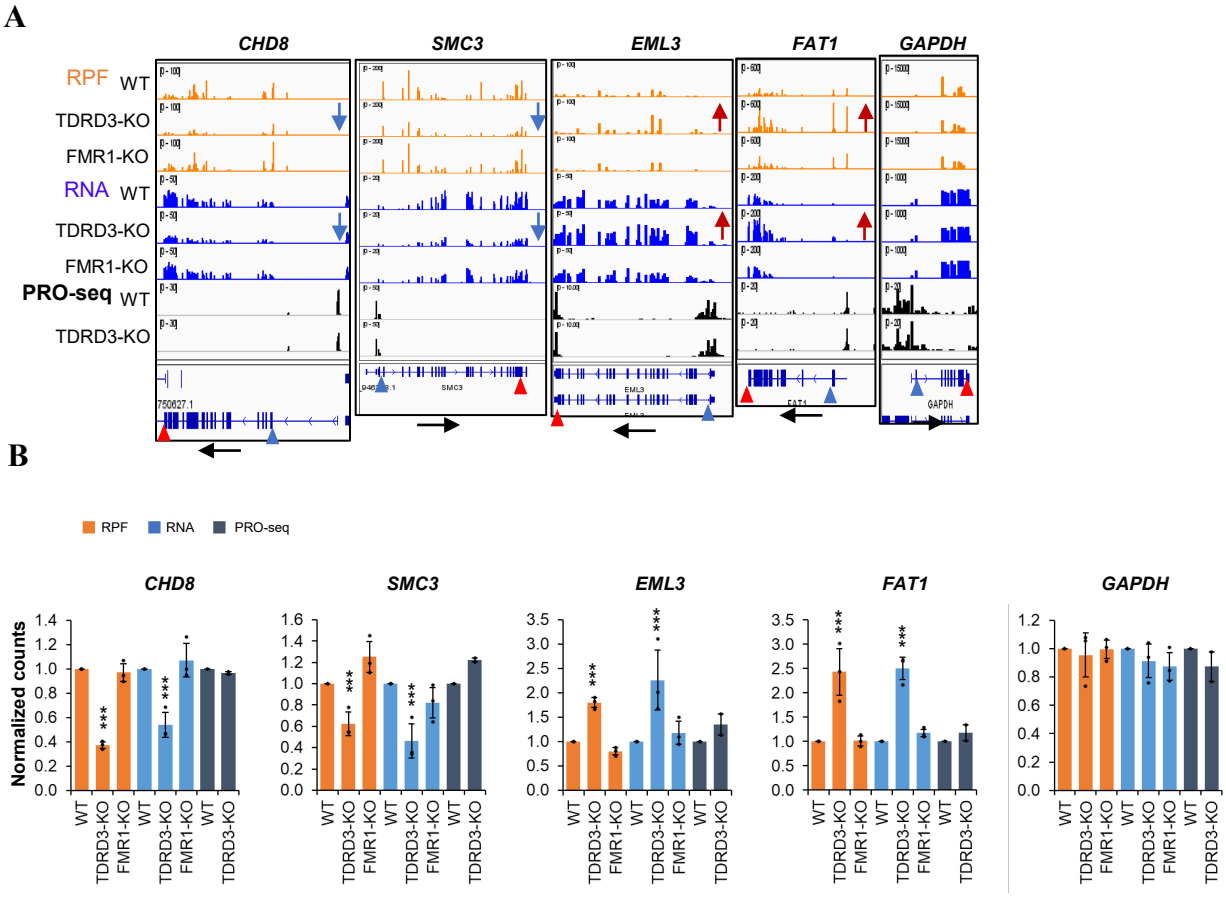

Figure 8. Multiple mental disorder risk genes are regulated by both TOP3B and TDRD3.

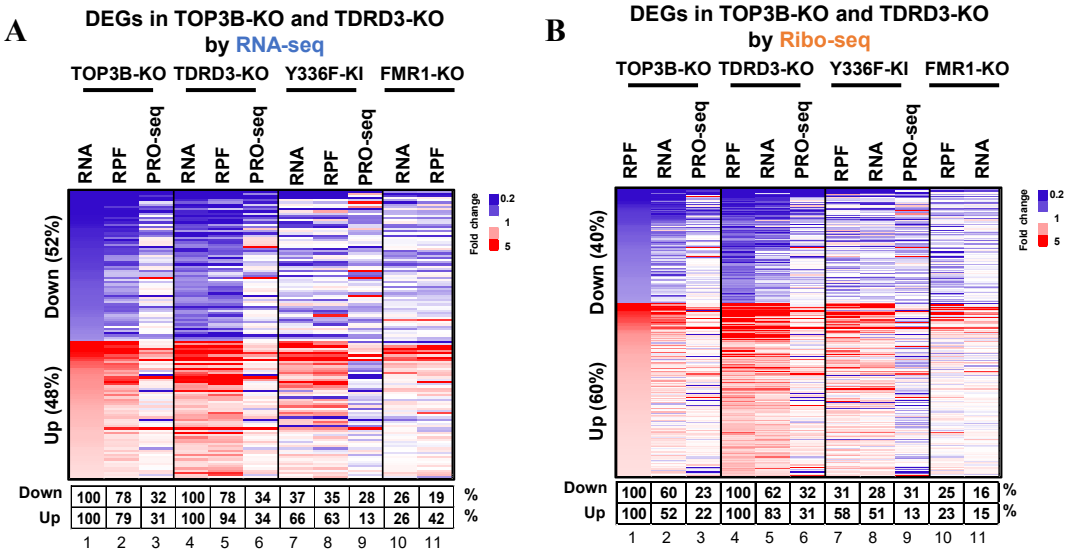

C

DEGs associated with autism or schizophrenia in both *TOP3B-KO* and *TDRD3-KO* HCT116 cells

RPF/RNA	Gene expression	autism	schizophrenia
RPF	down	***TTN***, *SATB2*, ***CHD8***, *SMC3, GALNT14, PER1, SBF1, PRR12*	*SATB2, VPS37B, TLE1, ME1, PRR12*
	up	*GRIN2B*, ***SYT1***, *BCORL1, IRF2BPL, GRIN1,* ***CEP290***, *STK39,* ***FAT1***, ***PTK7***	*GRIN2B,* ***BDNF***, ***INPP4B***, *MDK, ENKD1,* ***PDE4B***
RNA	down	*SBF1, DLX2, SATB2, MBD6*	*SATB2*
	up	***GRIN2B***, ***SYT1***, *STK39,* ***FAT1***, ***ALDH1A3***	***GRIN2B***, ***INPP4B***, ***BDNF***, *AIG1*

The genes in bold are regulated in topoisomerase catalytic activity dependent manner.

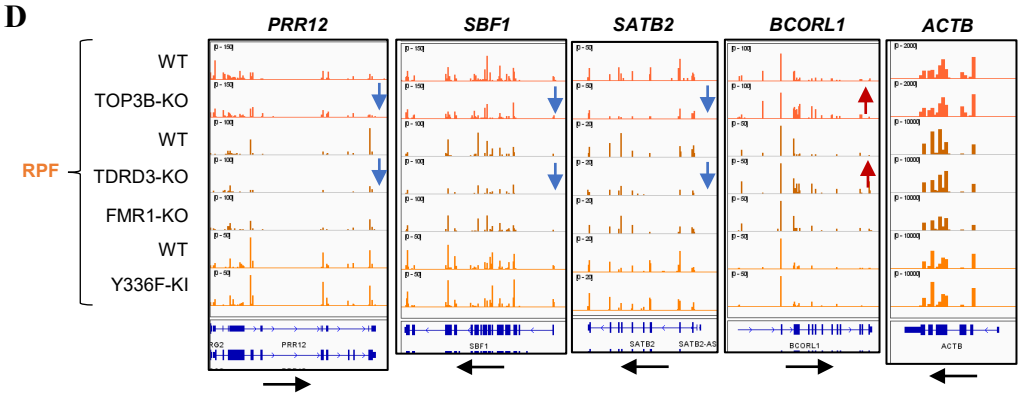

Figure 9. eCLIP-seq reveals that TOP3B prefers to bind coding region of long mRNAs and its binding stabilizes these mRNAs.

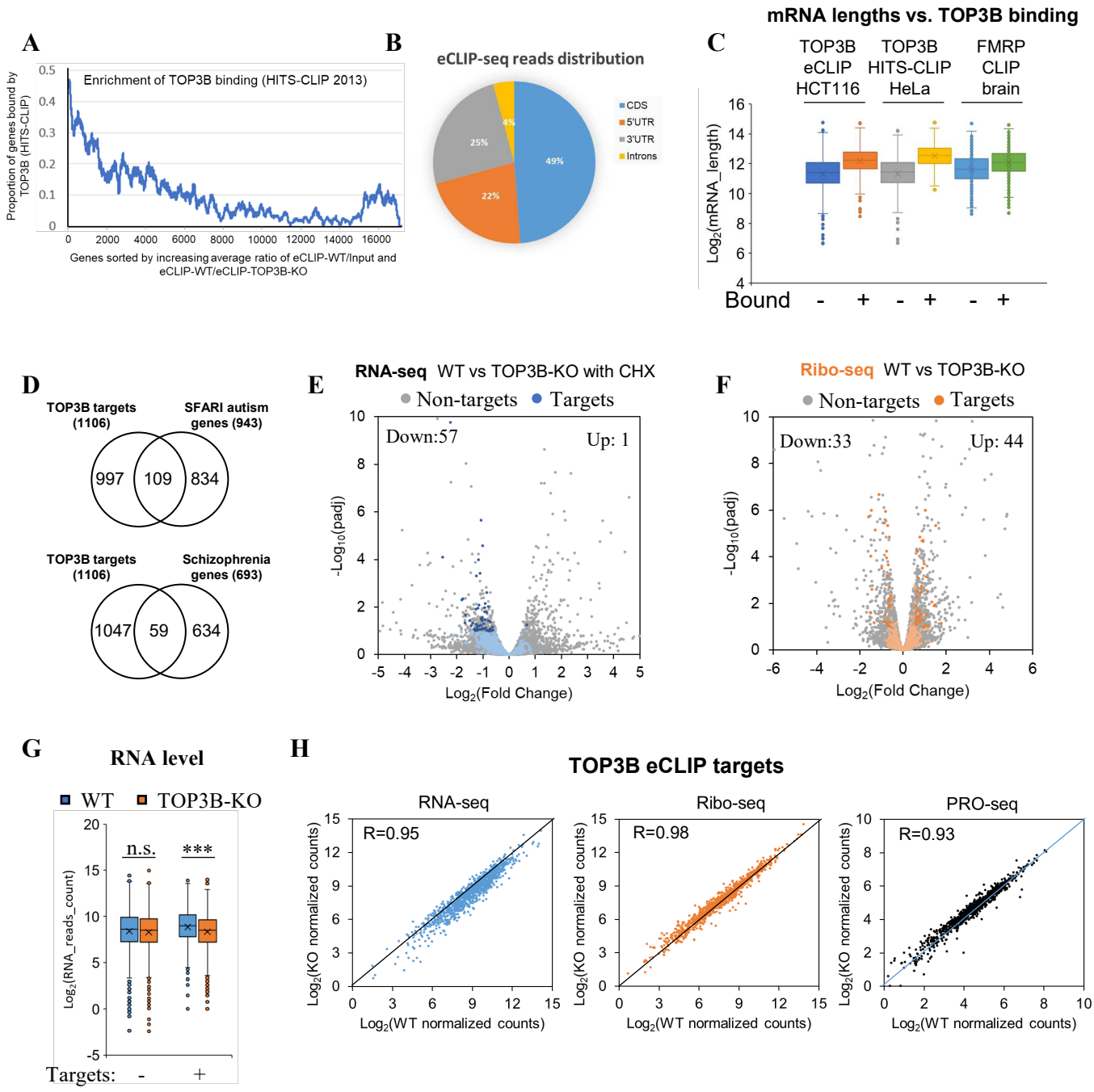

Figure 10. TOP3B stabilizes its bound mRNAs by topoisomerase activity independent manner.

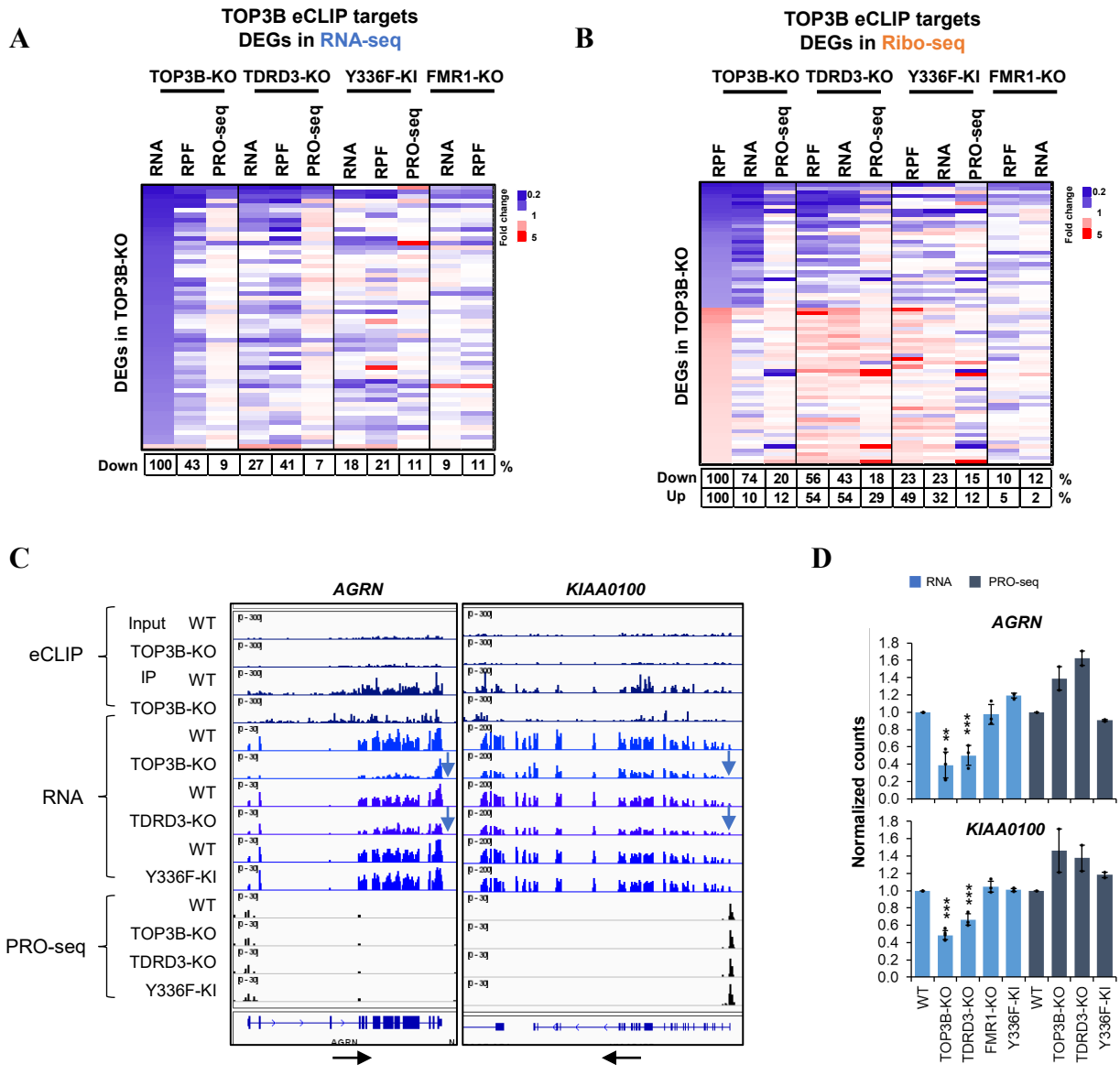

Figure 11. Models showing the roles of the TOP3B-TDRD3 complex in translation and mRNA stability.

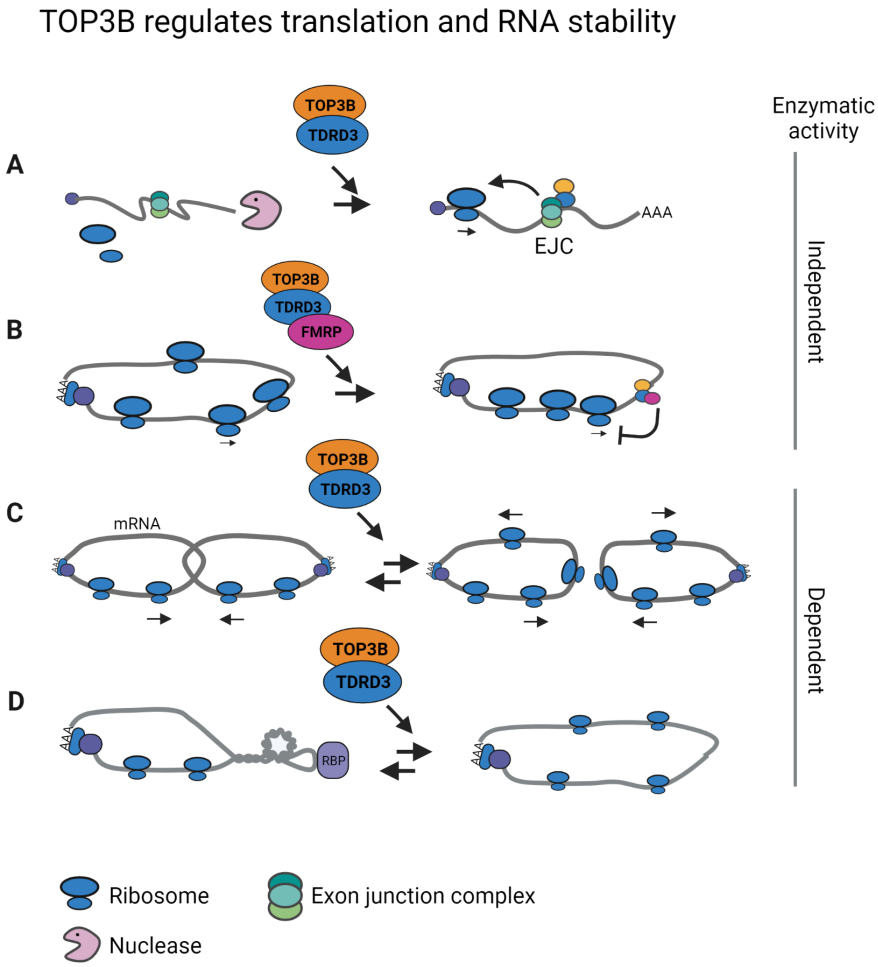

Supplementary Files

This is a list of supplementary files associated with this preprint. Click to download.

- 2.8.2022.SupplementaryFiguresS1S7.pdf
- TableS1.xlsx
- TableS2.xlsx
- TableS3.xlsx
- TableS4.xlsx
- TableS5.xlsx
- TableS6.xlsx
- TableS7.xlsx
- TableS8.xlsx
- TableS9.xlsx